An Inverse Algorithm To Estimate Thermal Contact Resistance

2005

Jennifer Gill
University of Central Florida

AN INVERSE ALGORITHM TO ESTIMATE THERMAL CONTACT RESISTANCE

by

JENNIFER REBEKAH GILL
B.S. University of New Mexico, 2000

A thesis submitted in partial fulfillment of the requirements
for the degree of Master of Science
in the Department of Mechanical, Materials and Aerospace Engineering
in the College of Engineering and Computer Science
at the University of Central Florida
Orlando, Florida

Fall Term
2005

ABSTRACT

Thermal systems often feature composite regions that are mechanically mated. In general, there exists a significant temperature drop across the interface between such regions which may be composed of similar or different materials. The parameter characterizing this temperature drop is the thermal contact resistance, which is defined as the ratio of the temperature drop to the heat flux normal to the interface. The thermal contact resistance is due to roughness effects between mating surfaces which cause certain regions of the mating surfaces to loose contact thereby creating gaps. In these gap regions, the principal modes of heat transfer are conduction across the contacting regions of the interface, conduction or natural convection in the fluid filling the gap regions of the interface, and radiation across the gap surfaces. Moreover, the contact resistance is a function of contact pressure as this can significantly alter the topology of the contact region. The thermal contact resistance is a phenomenologically complex function and can significantly alter prediction of thermal models of complex multi-component structures.

Accurate estimates of thermal contact resistances are important in engineering calculations and find application in thermal analysis ranging from relatively simple layered and composite materials to more complex biomaterials. There have been many studies devoted to the theoretical predictions of thermal contact resistance and although general theories have been somewhat successful in predicting thermal contact resistances, most reliable results have been obtained experimentally. This is due to the fact that the nature of thermal contact resistance is quite complex and depends on many parameters including types of mating materials, surface characteristics of the interfacial region such as roughness and hardness, and contact pressure

distribution. In experiments, temperatures are measured at a certain number of locations, usually close to the contact surface, and these measurements are used as inputs to a parameter estimation procedure to arrive at the sought-after thermal contact resistance. Most studies seek a single value for the contact resistance, while the resistance may in fact also vary spatially.

In this thesis, an inverse problem (IP) is formulated to estimate the spatial variation of the thermal contact resistance along an interface in a two-dimensional configuration. Temperatures measured at discrete locations using embedded sensors appropriately placed in proximity to the interface provide the additional information required to solve the inverse problem. A superposition method serves to determine sensitivity coefficients and provides guidance in the location of the measuring points. Temperature measurements are then used to define a regularized quadratic functional that is minimized to yield the contact resistance between the two mating surfaces. A boundary element method analysis (BEM) provides the temperature field under current estimates of the contact resistance in the solution of the inverse problem when the geometry of interest is not regular, while an analytical solution can be used for regular geometries. Minimization of the IP functional is carried out by the Levenberg-Marquadt method or by a Genetic Algorithm depending on the problem under consideration. The L-curve method of Hansen is used to choose the optimal regularization parameter. A series of numerical examples are provided to demonstrate and validate the approach.

ACKNOWLEDGMENTS

A major lesson to be learned from the sometimes-overwhelming tasks associated with completion of a thesis is that it is truly a collaborative effort. Throughout the process of research, writing, proofreading and eventual submittal, the final document is the product of many participants. Some of the participants contributed directly and some indirectly, some participated willingly and some were duped, but all provided valuable input and support. While I will attempt to acknowledge all who helped to complete this thesis, I'm sure that I will have forgotten someone. So to all who are listed below….and to all who helped but are not listed….a sincere thank you.

UCF faculty: Dr. Alain Kassab, Dr. Eduardo Divo, Dr. Nicholson. NASA Kennedy Space Center: Dr. Lisa Huddleston, David Huddleston, Joy Huff, Ivan Velez, David Kelley, Jeff Brink, Ed Markowski. My family and friends: Katie Grigg, Walter Gill, Alexander Morgan, Sara Palermo, and finally my kitties Francine, Vanessa, and Tigger.

TABLE OF CONTENTS

LIST OF FIGURES

LIST OF TABLES

LIST OF ACRONYMS/ABBREVIATIONS

BEM	Boundary Element Method
BIE	Boundary Integral Equation
FEM	Finite Element Method
GA	Genetic Algorithm
IP	Inverse Problem
RBF	Radial Basis Function
RMS	Root Mean Square

CHAPTER ONE: INTRODUCTION

Thermal systems generally feature composite regions that are mechanically mated. In general, there exists an often significant temperature drop across the interface between such regions which may be composed of similar or different materials. The parameter characterizing this temperature drop is the thermal contact resistance, $R''_{t,c} = \Delta T/q''$, which is defined as the ratio of the temperature drop, ΔT to the heat flux normal to the interface, q''. The thermal contact resistance is due to roughness effects between mating surfaces which cause certain regions of the mating surfaces to lose contact thereby creating gaps. In these gap regions, the principal modes of heat transfer are conduction across the fluid filling the gap and radiation across the gap surfaces. Moreover, the contact resistance is a function of contact pressure as this can significantly alter the topology of the contact region. Clearly, the thermal contact resistance is a phenomenologically complex function and can significantly alter prediction of thermal models of complex multi-component structures. Accurate estimates of thermal contact resistance are thus important in engineering calculations and find application in thermal analysis ranging from relatively simple layered and composite materials to more complex bio materials. There have been many studies devoted to the theoretical predictions of thermal contact resistance, for instance, (DeVaal et al 1987; Negus et al 1987; Marotta and Fletcher 2001; Muzychka et al 1996), and comprehensive reviews of previous work on thermal contact resistance can be found in (Yovanovich 1998; Madhusudana and Fletcher 1986; Blackwell et al 2000). Although general theories have been somewhat successful in predicting thermal contact resistances, most reliable results have been obtained experimentally. This is due to the fact that the nature of thermal

contact resistance is quite complex and depends on many parameters including types of mating materials, surface characteristics of the interfacial region such as roughness and hardness, and contact pressure distribution. In experiments, temperatures are measured at a certain number of locations, usually close to the contact surface, and these measurements are used as inputs to a parameter estimation procedure to arrive at the sought-after thermal contact resistance. Most studies seek a single value for the contact resistance, while the resistance may in fact also vary spatially.

In this thesis, an inverse problem (Beck et al 1985; Alifanov 1994; Kurpisz and Nowak 1995) is formulated to estimate the variation of the thermal contact resistance along an interface in two-dimensional configuration. Temperature measured at discrete locations using embedded sensors placed in proximity to the interface provide the information required to solve the inverse problem. The contact resistance is found by using a superposition method to determine sensitivity coefficients (Blackwell and Dowding 2002; Bialecki et al 2003) for specific temperature measurement points in the geometry. This serves to guide in the location of the measuring points. Temperature measured at these discrete locations are then used in a regularized least-squares problem to yield the contact resistance between the two mating surfaces. A boundary element method (BEM) (Brebbia et al 1985; Kassab and Wrobel 2000; Divo and Kassab 1997; Divo and Kassab 1998; Kassab et al 2005; Divo and Kassab 2003) is also used to solve for the temperature under current estimates of the contact resistance during the solution of the inverse problem. An analytical solution is derived to verify the BEM. The inverse problem is solved using sensitivity analysis and also via a regularized BEM Genetic Algorithm (GA) (Goldberg 1989) approach previously developed by the authors (Divo et al 2002). The L-curve method of Hansen and O'Leary (1993; Hansen 1992) is used to choose the

optimal regularization parameter. A series of numerical examples are provided to demonstrate the approach.

CHAPTER TWO: PROBLEM DEFINITION

In general the thermal contact resistance may vary spatially along the contact surface between mating regions. Most studies neglect that variation and rather seek a single value of the contact resistance as a function a certain parameters, such as temperature, contact pressure, and interfacial fluid. In this thesis, we consider an intermediate model, whereby the contact resistance is assumed to vary with position along a contact line in a 2-D configuration. We simulate a steady-state experiment seeking to characterize the unknown variation of the contact resistance.

The general configuration of interest is a two-dimensional region illustrated in Fig. 1. Two blocks of materials of different conductivities k_u and k_b are joined at an interface located at a level $y = l$. The top and bottom surfaces of the sample are kept at constant but different temperatures, and the sides are modeled as adiabatic. In practice, temperature measurements are carried out at a series of locations close to the interface, here, illustrated by solid dots in Fig. 1 and the purpose of the inverse problem is to identify the functional variation of $R''_{t,c}$. In this thesis, these measurements including certain levels of uncertainties in the measurements are simulated numerically and these are considered inputs to the inverse problem.

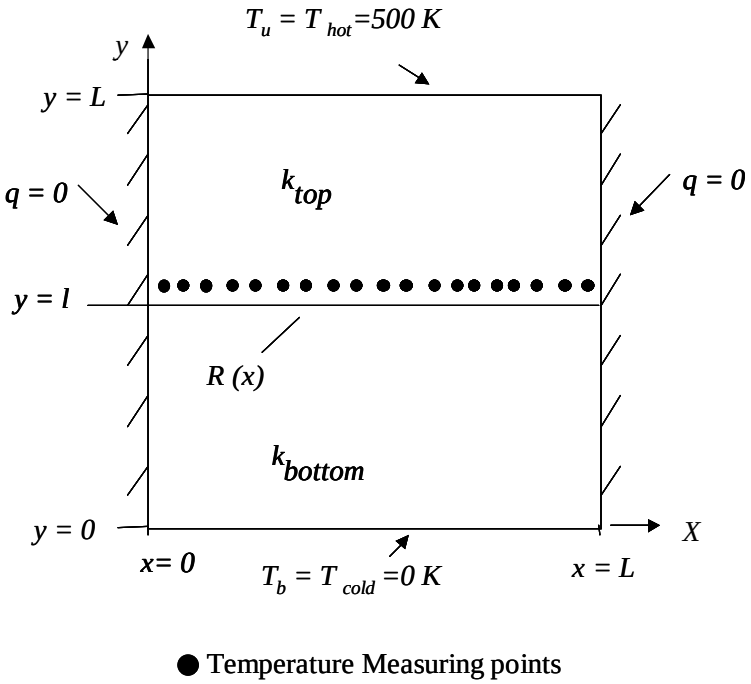

Figure 1. Illustration of the model of a simulated steady-state experiment to retrieve thermal contact resistance

It is instructive to broadly describe inverse problems and contrast these to traditional or forward problems. Analysis of engineering field problems can broadly be classified as either forward or inverse. Forward problems are most commonly encountered, and in a forward problem, the following are explicitly specified:

1. Governing equation for field variable
2. Physical properties
3. Boundary conditions
4. Initial conditions
5. System geometry

The purpose of solving the forward problem is to determine the field variable given these inputs. In contrast, in an inverse problem, the following are explicitly specified:

1. Part of conditions 1-5 in a forward problem
2. An over-specified condition

The purpose of solving the inverse problem is to find the unknown in conditions 1-5 of the forward problem, using the over-specified condition. Typically, the over-specified condition is provided by measuring a field variable at the exposed boundary or at the interior. Inverse problems are ill-posed by nature and very sensitive to noise input measurement. As such, some stabilization (regularization) is required, see Tikonov and Arsenin (1977), Beck and Blackwell (1885), Alifanov (1994), and Kurpisz and Nowak (1995).

In our case, the inverse problem is a thermal one with the field variable identified as the contact resistance with the geometry, thermal conductivity and boundary conditions fully specified. A typical inverse problem algorithm consists of the following three components:

1. An objective function providing a quantitative measure between the difference of the predicted temperature at the measuring points and the measured temperature there given the current estimate of the thermal contact resistance distribution: we will define a regularized least-squares functional.
2. A minimization algorithm to automatically update the estimated heat transfer coefficient distribution in the process of minimizing the objective function: we will use the Levenberg-Marquadt method or a genetic algorithm depending on the problem at hand.
3. A forward problem solver: we will use either an analytical solution when possible or alternatively a numerical method to provide flexibility in geometric modeling and in the

case of non-linear variation of the contact resistance that preclude an analytical solution. In the latter case, we use the boundary element method (BEM) in particular.

Each of the components of the formulation is described in turn in the following chapters.

CHAPTER THREE: THE INVERSE PROBLEM

There are two formulations developed in this thesis for the solution of the inverse problem under consideration. Both define a quadratic functional and minimize that functional in order to determine the unknown contact resistance. The first method requires the computation of sensitivities (elements of the Jacobian of the objective function) while the second method only requires functional evaluations. Each of these formulations is now developed in detail.

Modeling of the Spatial Variation of the Contact Resistance

In solving for the contact resistance, one may solve directly for the values of the contact resistance $R''_{tc}(x)$ at discrete locations $(x_1, x_2, ...x_M)$. This can lead to problems in the inverse formulation in that a relatively large number of unknowns must be resolved. It is often good practice to parametrize the contact resistance prior to solution, thereby reducing the number of unknowns and providing a certain degree of flexibility in the modeling of the variability of the contact resistance. In such a case, we use radial basis function (RBF) interpolation and represent the contact resistance as $R''_{t,c}(x) = \sum_{j=1}^{N} R_j f_j(x, x_j)$. Here we use f_j as the radial distance between the expansion (anchor) point and any field point; $f_j = 1+r$. In such a case the expansion coefficients R_j become the unknowns. These are solved by collocation at the discrete locations $(x_1, x_2, ...x_N)$, where in inverse problem application N is taken as a small number to reduce the number of sought-after unknowns. A typical RBF interpolation of a complex thermal contact resistance is displayed in Figure 2, where N is taken as 11.

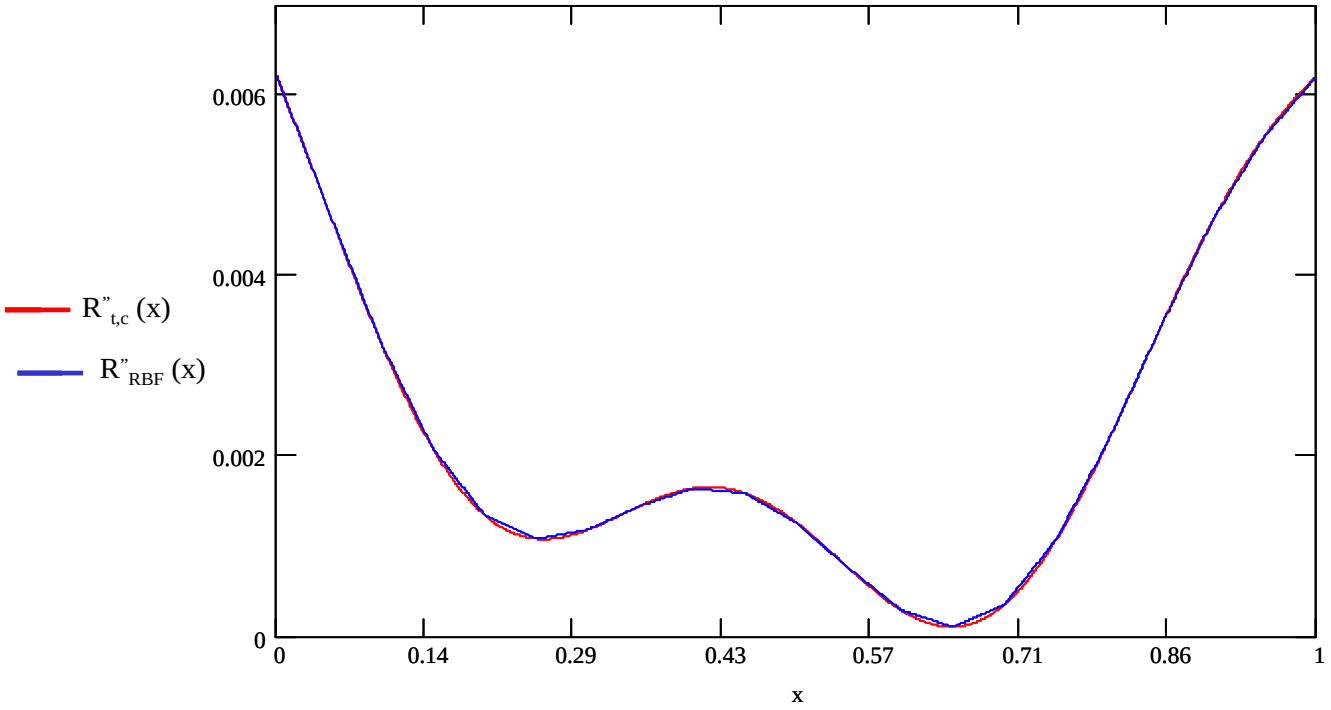

Figure 2. RBF interpolation for a typical $R''_{t,c}(x)$ distribution using N=11.

Sensitivity-Based Inverse Formulation

In this approach to the inverse problem, the sensitivities are obtained using a notion borrowed from Zhang et al (1997) and Bialecki et al (2003). This technique requires that the measurements, in our case temperatures, are linearly dependent on the sought-after variables in the inverse problem, in our case the discrete values of the contact resistance. Here a series of forward problems are solved to evaluate the temperature at the measurement locations as a function of a unit value of contact resistance at x-locations along the contact surface (resistance

measuring points). For this purpose, an analytical solution may be used if available or a numerical method may be used in general.

The notion here is that the vector of measured temperatures can be expressed in a linear relation to the thermal contact resistance as $\underline{T}_{measuring\ points} = \underline{T}_{baseline} + \underline{\underline{S}}\,\underset{\sim}{R}''$. The sensitivities, S_{ij}, defined as $S_{ij} = \frac{\partial T_i}{\partial R_j}$ can thus be evaluated numerically evaluated. The first column of the matrix, $\underline{\underline{S}}$, is the corresponding sensitivities for all thermocouple locations when there is a perturbation at a resistance $R(x_1)$, and zero resistance at all other x locations. The second column is the same information for a perturbation resistance at the resistance $R(x_2)$ and zero resistance at all other locations. Thus the entries of the matrix represent the sensitivity of the thermocouple locations to resistance at each of the measurement locations. The locations $(x_1, x_2, ...x_N)$ used in generating the sensitivity matrix may be physical locations where contact resistance is sought, or selected points used in a parametric model of the contact resistance, see for instance (Divo et al 2002). In any case, we refer to these as anchor points. The results can be displayed in a sensitivity matrix, as shown in Figs. 3 and 4.

A baseline temperature distribution was computed by allowing the resistance to be zero everywhere. The baseline temperature distribution was subtracted from each measurement point run and divided by r(x) to determine the sensitivity. For this work, a constant value of perturbation resistance is used and set to $r = 0.0005 Km^2/W$ for scaling purposes as a unit perturbation is much larger than any expected value of actual contact resistance and would lead to very high baseline temperature values and consequently numerical issues in solving the inverse problem.

With the matrix $\underline{\underline{S}}$ of the sensitivities in hand, the calculated solution to the linear forward model for the temperatures at the measurement points for any distribution of thermal contact resistance values becomes simply

$$\underset{\sim}{T}_{calculated} = \underset{\sim}{T}_{baseline} + \underline{\underline{S}}\,\underset{\sim}{R} \tag{1}$$

where $\underset{0\angle}{R}$ would be known values of the contact resistance at the anchor points. Because of the linearity, this approach is valid if the baseline case is not far from the actual case. An example of the sensitivity matrix is provided below for the problem under consideration.

860	750	238	186	74	68	30	30	10	28	14	8	4	4	2	2	0	2	0
512	1024	452	304	108	92	40	38	12	34	16	8	4	4	2	2	2	2	0
238	660	696	632	194	148	58	52	16	48	22	12	6	6	2	4	2	2	2
126	304	432	958	426	280	96	82	22	74	32	16	8	8	4	4	2	2	2
74	160	194	620	680	616	188	142	32	126	50	22	10	10	6	6	2	4	2
46	92	100	280	422	946	420	276	52	240	84	32	14	14	8	8	4	4	2
30	58	58	144	188	614	676	612	94	520	162	48	22	22	10	10	6	6	4
22	38	36	82	94	276	420	944	188	820	358	78	32	32	14	16	8	8	6
14	26	24	50	54	140	186	612	328	644	590	140	54	48	22	22	12	12	8
10	18	16	32	34	80	94	274	446	464	446	274	94	80	34	32	16	18	10
8	12	12	22	22	48	54	140	590	270	328	612	186	140	54	50	24	26	14
6	8	8	16	14	32	32	78	358	134	188	944	420	276	94	82	36	38	22
4	6	6	10	10	22	22	48	162	74	94	612	676	614	188	144	58	58	30
2	4	4	8	8	14	14	32	84	46	52	276	420	946	422	280	100	92	46
2	4	2	6	6	10	10	22	50	30	32	142	188	616	680	620	194	160	74
2	2	2	4	4	8	8	16	32	20	22	82	96	280	426	958	432	304	126
2	2	2	4	2	6	6	12	22	16	16	52	58	148	194	632	696	660	238
0	2	2	2	2	4	4	8	16	12	12	38	40	92	108	304	452	1024	512
0	2	0	2	2	4	4	8	14	10	10	30	30	68	74	186	238	750	860

Figure 3. Sensitivity matrix S (W/m^2). The columns correspond to the measurement location, the rows to the anchor point location, shown here for a location 0.00625m above the interface region

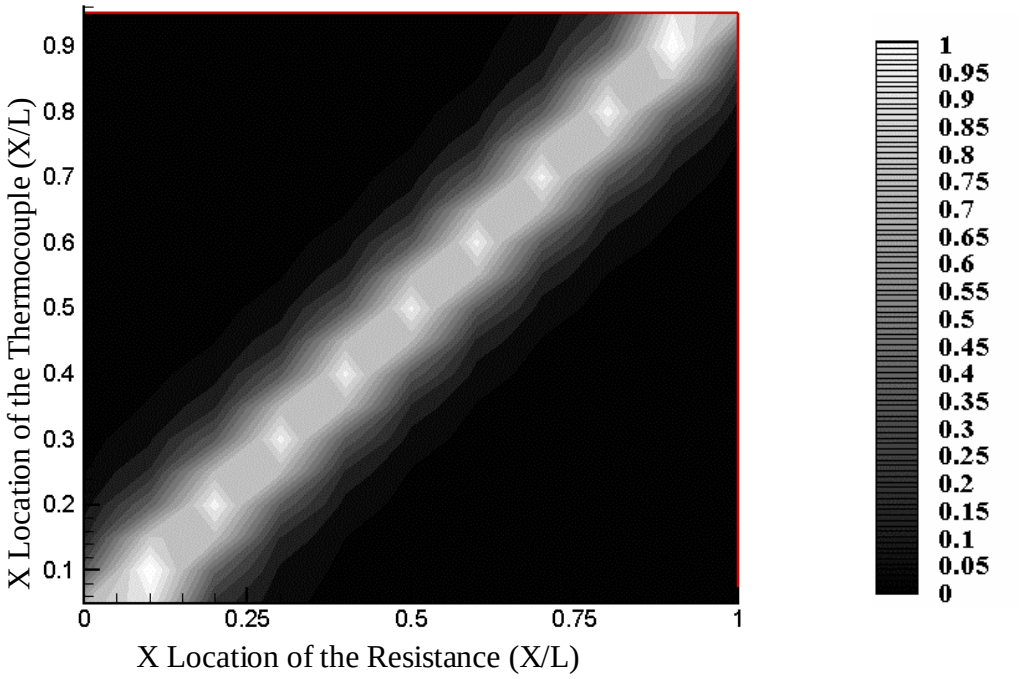

Figure 4. Plot of the sensitivity matrix. Shown here for a location 0.00625m above the interface region. On the gray scale white is high sensitivity and black is zero sensitivity.

With the sensitivity matrix in hand, an inverse problem may now be formulated. When the number of thermocouples equals the number of resistance anchor points, an unknown $\underset{\sim}{R}$ can be determined for observed temperatures from the simple inversion of Equation 14:

$$\underset{\sim}{J}(\underset{\sim}{R}) = \underline{\underline{S}}^{-1}\left(\underline{T}_{obs} - \underline{T}_{baseline}\right) \tag{2}$$

However, this is often leads to unacceptable results due to the fact that *S* is ill-conditioned. Thus input noise in the measurements usually leads to values of R with very large errors. Thus, in solving inverse problems, many more measurements are taken than the number of sought-after unknowns and a least-squares formulation is used to find the unknown $\underset{\sim}{R}$:

$$J(\underset{\sim}{R}) = (\underline{\underline{S}}^T \underline{\underline{S}})^{-1} \underline{\underline{S}}^T (\underset{\sim}{T}_{obs} - \underset{\sim}{T}_{baseline}) \tag{3}$$

supplemented by a regularization (stabilizing) scheme. One of the best known regularization methods for inverse problems is Tikhonov regularization (Hansen 1992), also called damped least squares shown in Fig. 5.

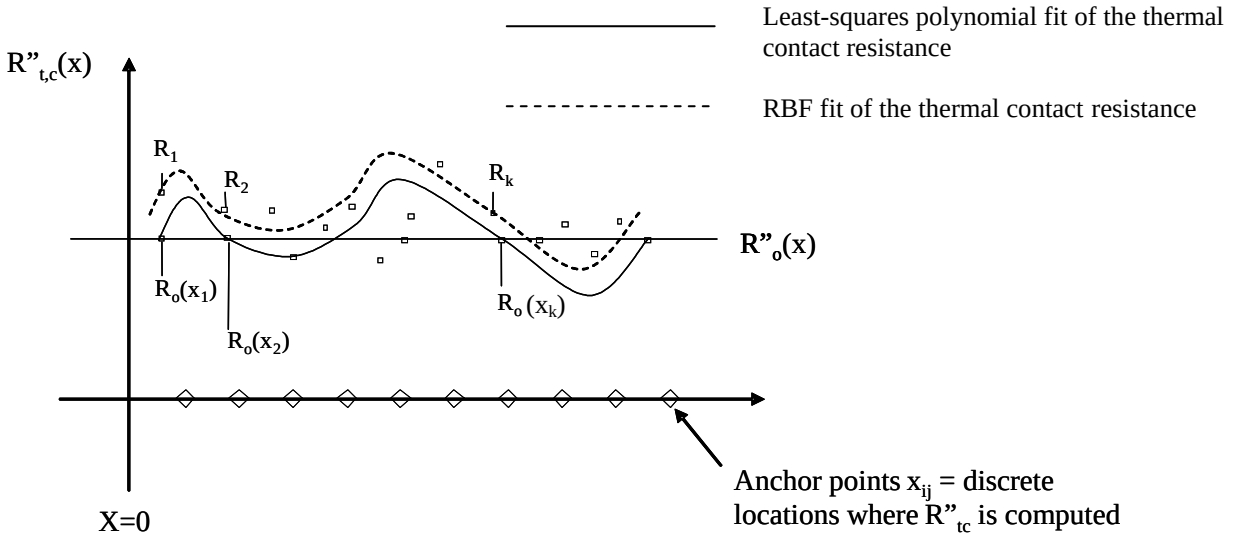

Figure 5. An example of a least-squares fit polynomial approximation through the current values of the contact resistance, here taken as a constant.

A first order regularized solution is defined using the following augmented least squares functional (Hansen and O'Leary 1993).

$$\min\left\{\left\|\underline{\underline{S}}\,\underset{\sim}{R} - \left(\underset{\sim}{T}_{obs} - \underset{\sim}{T}_{baseline}\right)\right\|^2 + \beta\left\|\underset{\sim}{R} - \underset{\sim}{R}_0\right\|^2\right\} \tag{4}$$

The parameter β controls how much weight is given to minimization of $\left\| \underset{\sim}{R} - \underset{\sim 0}{R} \right\|$ relative to minimization of the residual norm. Traditionally, $\underset{\sim 0}{R}$ is taken as a constant, and this does not provide flexibility in damping spatially-varying functions. To overcome this limitation, we take $\underset{\sim 0}{R}$ as a least-squares fit polynomial approximation through the current values of the contact resistance, effectively bringing the RBF approximation towards its mean value at the RBF anchor points. Since $\underset{\sim 0}{R}$ is not known, it is initially set to zero in order to find $\underset{\sim}{R}$ as a result of the first iteration. Subsequently, $\underset{\sim 0}{R}$ is updated in all future iterations. The minimization of this least squares problems is accomplished via the Levenberg-Marquadt method.

Genetic Algorithm-Based Inverse Problem Solution

We have carried the idea of regularized least squares forward into the BEM/GA method that does not require evaluation of the sensitivities and that does not require a linear relationship between the temperature measurements and the sought-after values of the contact resistance. Moreover, the GA minimization technique promises to find the global minimum within the search space. We minimized an objective function Z extended to include the discrepancy between computed $T_{c,i}$ and measured temperatures $T_{m,i}$ under current estimate of the contact resistance at anchor points $R_{c,i}$. Following the sensitivity-based developments, the objective function is regularized with respect to the running least-squares fit of the contact resistance at the anchor points $R_{m,i}$ as:

$$Z(\underset{\sim}{R}) = \left(\sum_{1}^{M} \left(T_{m,i} - T_{c,i} \right)^2 \right)^{\frac{1}{2}} + \beta \left(\sum_{1}^{M} \left(R_{m,i} - R_{c,i} \right)^2 \right)^{\frac{1}{2}} \tag{5}$$

This function is then minimized in an effort to arrive at a contact resistance which best fits the measurement data. We use a genetic algorithm (GA) (Goldberg 1989) to minimize Eqn. 5. It is noted that Eqn. 5 is different in form than from 4. This is because Eqn. 5 is better suited for implementation in the existing GA implementation. Better results are expected from the BEM/GA method because it is not necessary to assume a linear perturbation about a baseline case as was taken by the sensitivity approach. Thus, more general dependencies of the thermal contact resistance can be pursued, including temperature dependence. However, this is left to future studies.

Genetic algorithms are non-gradient based optimization algorithms that use random searches mimicking natural selection rules of evolution. Actually, GA's maximize objective functions as they naturally seek the "best fit." Thus the objective function computed by the GA is (Divo et al 2002):

$$Z_{GA}(\underset{\sim}{R}) = \frac{1}{Z(\underset{\sim}{R})} \tag{6}$$

Traditional optimization processes such as hill-climbing, nonlinear dynamic programming, and non-linear simplex algorithms have been widely used for optimization. However, a common feature shared by all these schemes is that they are local in scope. The optima they seek are the best in a neighborhood of the starting point. Once a minimum is reached, a new starting point has to be set-up in order to seek the possibility of a better solution.

Optimization schemes based on random variation such as evolutionary algorithms answer some of the short-comings of classical minimization techniques. The most common of such techniques include evolutionary strategies, evolutionary programming, and genetics algorithms (GA's). All of these schemes possess a common characteristic: they each involve reproduction, random variation, competition, and selection of contending individuals in a population within a given environment. Genetic algorithms (GA) are robust adaptive search techniques that mimic the idea of Darwinian evolution, Goldberg (1989), and use natural selection rules to investigate highly complex multi-dimensional problems. GA's have been successfully applied to a wide range of optimization problems implicit to most inverse formulations. Some advantages of GA's over classical optimization include: (1) no need for sensitivity coefficient evaluation as optimization is performed only by objective function evaluation, (2) based on randomness of optimization operators at each generation stage increasing the likelihood of finding several or even a global minimum, (3) continuity of the function or its derivatives is not required. Finding a global minimum is by no means assured by adopting a GA, and proof of a global minimum relies on convexity of the objective function. However, it can certainly be stated that a GA increases the likelihood of finding such a minimum, and, in the least, GA's provide an automated and logical manner to search the parameter landscape for multiple minimae (Divo et al 2002).

The GA optimization process begins by setting a random set of possible solutions, called the population, with a fixed initial size or number of individuals. Each individual is defined by optimization variables and is represented as a bit string or a chromosome (see Fig. 6 below).

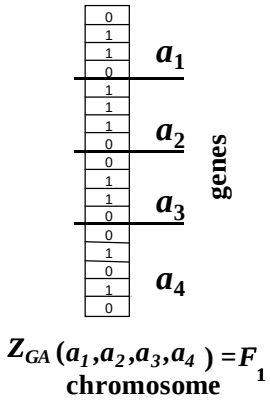

Figure 6. Individual in the population characterized by four parameters (genes) encoded in a chromosome yielding the individual's fitness value F_1 (Divo et al 2002)

An objective function, Z_{GA}, is evaluated for every individual in the current population defining the fitness or their probability of survival. At each iteration of the GA, the processes of selection, cross-over, and mutation operators are used to update the population of designs. A selection operator is first applied to the population in order to determine and select the individuals that are going to pass information in a mating process with the rest of the individuals in the population. This mating process is called the crossover operator, and it allows the genetic information contained in the best individuals to be combined to form offsprings. Additionally, a mutation operator randomly affects the information obtained by the mating of individuals. This is a crucial step for continuous improvement (Divo et al 2002).

A series of parameters are initially set in the GA code, and these determine and affect the performance of the genetic optimization process. The number of parameters per individual or optimization variables, the size of the bit string or chromosome that defines each individual, the number of individuals or population size per generation, the number of children from each mating, the probability of crossover, and the probability of mutation are among the parameters

that control the optimization process. This set of operations is carried out generation after generation until either a convergence criterion (a preset level of acceptable fitness) is satisfied or a maximum number of generations is reached. It is also important to point out that three important features distinguish GA's from the others evolutionary algorithms, namely: (1) binary representation of the solution, (2) the proportional method of selection, and (3) mutation and crossover as primary methods of producing variations (Divo et al 2002).

In nature, the properties of an organism are described by a string of genes in the chromosomes. Therefore, if one is trying to simulate nature using computers one must encode the design variable in a convenient way. We adopt a haploid model using a binary vector to model a single chromosome. The length of the vector is dictated by the number of design variables and the required precision of each design variable. Each design variable has to be bounded with a minimum and a maximum value and in the process the precision of the variable is determined. The number of divisions used in the discretization has to be integer power of two. This procedure allows an easy mapping from real numbers to binary strings and vice versa. This coding process represented by a binary string is one of the distinguishing features of GA's and differentiates them from other evolutionary approaches. The haploid GA's place all design variables into one binary string, called a chromosome or off-spring. The information contained in the string of vectors comprising the chromosome characterizes an individual in a population. In turn, each individual is equipped with a given set of design variables to which corresponds to a value of the objective function. This value is the measure of "fitness" of the individual design. In GA's, poorly fit designs are not discarded, rather they are kept, as in nature, to provide genetic diversity in the evolution of the population. This genetic diversity is required to provide forward

movement of the population during the mating, cross-over, and mutation processes which characterize the GA (Divo et al 2002).

The initial population size may grow or diminish to mimic actual biological systems. However, in the GA used here, the population size is not allowed to change while the program is running. Once the population size is fixed, the algorithm initializes all of the chromosomes. This operation is carried out by assigning a random value of 0 or 1 for each bit contained in each of the chromosomes. After initializing the population, evaluation of the fitness of each individual is performed by computing the objective (or fitness) which of course represents a set of possible solutions. Having the values of the objective function for each individual, the selection process can be started. First values of the fitness function for each individual have to be added, and then the probability of being a selected individual is calculated as the ratio between the value of the fitness function of each individual and the sum of all objectives function values. This is given by:

$$P_{selected} = \frac{Fitness(v_i)}{\sum_{i=1}^{pop-size} Fitness(v_i)} \tag{7}$$

where v_i is i-th member of the population, and Fitness(v_i) is the measure of the fitness of that member under its currently evolved parameter set configuration. A weighted roulette wheel is generated, where each member of the current population is assigned a portion of the wheel in proportion to its probability of selection. The wheel is spun as many times as there are individuals in the population to select which members mate. Obviously, some chromosomes would be selected more than once, where the best chromosomes get more copies, the average stay even, and the worst die off. Once selection has been applied, cross-over and mutation occur

to the surviving individuals. These operations further expand genetic diversity in the current population. All other probabilities referred to in the description of the GA adopted in this paper are computed in an analogous fashion as the selection probability (Divo et al 2002).

The probability of crossover P_c is an important parameter that defines the expected population size P_c•pop-size of chromosomes which undergoes crossover operation. This is a mating process that allows individuals to interchange intrinsic information contained in the chromosomes. The operation may be implemented in two steps: (1) a random selection based on the probability of crossover is performed to obtain pairs of individuals, and (2) a random number is generated between the first position of the binary vector and the last one, to indicate the location of the crossing point which delineates the location about which genetic information is interchanged between two chromosomes (Divo 2002 et al).

The mutation operator is the final operator implemented. The probability of mutation P_m gives the expected number of mutated bits and every bit in all chromosomes in the whole population has an equal chance to undergo mutation: switch of a bit from 0 to 1 or vice-versa. This process is implemented by generating a random number within the range (0...1) for each bit within the chromosome. If the generated number is smaller than P_m the bit is mutated. When the mutation is done on a bit-by-bit basis is called the creep mutation. Another type of mutation is the jump mutation which is applied to an individual selected to be mutated from this perspective. In this case all bits within the chromosome are switched from 0 to 1 and vice-versa. Following selection, crossover and mutation the new population is ready for its next evolution until the convergence criteria "fitness" is reached. It is the very nature of the binary representation of the design variables of the objective function and the random search process which provide yet another but implicit degree of regularization in this optimization process. The sensitivity of the

objective function can be tuned depending on the size of each element of the chromosome. Thus, low bit representation is insensitive to large variations in input (regularized but may lead to poor solution due to low resolution), while high bit representation is sensitive to large variations in input (not regularized and therefore may lead to poor solution as well). There is a range of bit size which produces a regularized and sensitive response leading to stable solutions (Divo et al 2002).

This completes the description of the inverse problem formulations considered in this thesis. Attention is now given to the analytical and numerical solution of the forward problem and, subsequently, numerical validation results will be presented.

CHAPTER FOUR: ANALYTICAL SOLUTION FOR CONDUCTION WITH CONTACT RESISTANCE

In certain applications, the contact resistance does not depend on the temperature and geometry is regular so that the problem geometry can be framed in a separable coordinate system and such a situation lends itself to the use of an analytical solution to the forward problem. The forward problem for the problem illustrated above is formulated considering the upper block temperature $T_u(x,y)$ and the lower block temperature $T_b(x,y)$ as:

$$
\begin{aligned}
&(a)\ \nabla^2 T_u = 0 \\
&(b)\ \nabla^2 T_b = 0 \\
&(c)\ \frac{\partial T_u(0,y)}{\partial x} = \frac{\partial T_u(L,y)}{\partial x} = \frac{\partial T_b(0,y)}{\partial x} = \frac{\partial T_b(L,y)}{\partial x} = 0 \\
&(d)\ k_u \left.\frac{\partial T_u(x,y)}{\partial y}\right|_{y=l} = k_b \left.\frac{\partial T_b(x,y)}{\partial y}\right|_{y=l} \\
&(e)\ k_b \left.\frac{\partial T_b(x,y)}{\partial y}\right|_{y=l} = \frac{T_u(x,l) - T_b(x,l)}{R(x)}
\end{aligned}
\tag{8}
$$

where, R(x) is the spatially varying contact resistance. A general analytical solution can be derived for the temperature distribution on the upper block and on the lower block by satisfying the governing equations and boundary conditions specified in Eqn. 8a through Eqn. 8e, leading to:

$$
T_u(x,y) = (T_{hot} - T_{cold})\left[1 - \frac{k_b}{k_u} c_0 \left(1 - \frac{y}{L}\right) - \frac{k_b}{k_u} \sum_{n=1}^{\infty} c_n \cos\left(\frac{n\pi}{L} x\right) \sinh\left(n\pi - \frac{n\pi}{L} y\right)\right] \tag{9}
$$

and

$$T_b(x,y) = (T_{hot} - T_{cold})\left[c_0 \frac{y}{L} + \sum_{n=1}^{\infty} c_n \cos\left(\frac{n\pi}{L}x\right)\sinh\left(\frac{n\pi}{L}y\right)\right] \quad (10)$$

The unknown coefficients, c_n's, can be explicitly computed by applying the temperature 'jump' condition at the interface, Eqn. 8e, and using the orthogonality properties of the $\cos\left(\frac{n\pi}{L}x\right)$ eigenfunctions. Each term, c_n, is computed through an independent superposition process. Details of the derivation are provided in the appendix. This approach can be generalized to as many terms as necessary to ensure convergence of the series. In our work we set the upper limit in the summation to 20 terms to generate the numerical results used in the sensitivity analysis.

CHAPTER FIVE: BOUNDARY ELEMENT MODEL FOR CONDUCTION WITH CONTACT RESISTANCE

The Boundary Element Method (BEM) is a numerical implementation of boundary integral methods for solution of field problems. The BEM is now a well established numerical method which can be efficiently used to solve heat conduction problems in linear and non-linear media as well as non-homogeneous media using boundary-only discretization. In addition to boundary-only discretization, a distinct feature of BEM is that unknowns which appear in the BEM formulation are the surface temperature and heat flux.

Assuming that the conductivity is constant, the Laplace equation governs the temperature field in each region in Fig. 1. Should the conductivity significantly vary as a function of temperature, the Kirchhoff transform can be used to linearize the heat conduction equation to the Laplace equation in the Kirchhoff transform (Brebbia et al 1985; Kassab and Wrobel 2000). In the direct BEM used in this thesis, the governing equation is first converted to a boundary integral equation (BIE) by: (1) multiplying the governing equation by a test function G(x,ξ), (2) integrating over the spatial domain and using Green's second identity, and (3) invoking properties of the Green free-space solution identified as the test function G(x,ξ), resulting in

$$C(\xi)T(\xi) = \oint_{\Gamma} \left[H(x,\xi)T(x) - q(x)G(x,\xi) \right] d\Gamma \tag{11}$$

This BIE is valid for boundary or interior points. Here, Γ is the domain boundary of a domain Ω, $\frac{\partial}{\partial n}$ denotes the normal derivative with respect to the outward-drawn normal,

$H(x,\xi) = -k\partial G(x,\xi)/\partial\eta$ and $q(x,t) = -k\partial T(x)/\partial\eta$. The free term, $C(\zeta)$ is 1, for $\xi \in \Omega$ and is equal to the internal angle subtended at a point on the boundary, $\xi \in \Gamma$, divided by 2π degrees in 2D and 4π steradian in 3D. The Green free space solution for the Laplace equation solves the adjoined diffusion equation perturbed in free space by a Dirac delta function located at the source point $x = \xi$ and is, $G(x,\xi) = -\ln r / 2\pi k$ in 2-D with $r = |x - \xi|$. The boundary Γ is discretized using N boundary elements,and the flux and temperature are discretized over the boundary to lead to the following form,

$$C_i T_i + \sum_{j=1}^{N} H_{ij} T_j = \sum_{j=1}^{N} G_{ij} q_j \tag{12}$$

where the coefficients H_{ij} and G_{ij} involve integrals of products of $H(x,\xi_i)$ and $G(x,\xi_i)$ with the appropriate shape function over the boundary element j. These are numerically evaluated by Gauss-type quadratures. The discretized BIE relates the temperature at any collocation point ξ_i (either on the boundary or in the domain) with boundary temperatures and heat fluxes. Collocating at ξ_i $H(x,\xi_i)$ boundary nodes $(i = 1,..,N)$ the above yields the standard form

$$[H]\{T\} = [G]\{q\} \tag{13}$$

The above is re-arranged into the standard algebraic form $[A]\{x\} = \{b\}$ by imposing boundary conditions. Applying the BEM formulation to the 2-region problem, we arrive at two equations

$$\begin{aligned} \left[H^I\right]\{T\}^I &= \left[G^I\right]\{q^I\} \qquad \text{for region I} \\ \left[H^{II}\right]\{T\}^{II} &= \left[G^{II}\right]\{q^{II}\} \qquad \text{for region II} \end{aligned} \tag{14}$$

at the contact region which is the interface of regions I and II. Here, flux continuity and temperature jump conditions are enforced:

$$\begin{aligned} q_j^I &= -q_j^{II} \qquad \text{for } j = 1, 2..N_{\text{int}} \\ T_j^I - T_j^{II} &= q_j^I R_{t,c}^{"}(x_j) \quad \text{for } j = 1, 2..N_{\text{int}} \end{aligned} \tag{15}$$

where N_{int} is the number of interfacial nodes. In standard BEM, Eqn. 14 is assembled into a global matrix using the interfacial conditions of Eqn. 15, and the subsequent equations are solved. When multiple regions are involved, the global matrix is structured with many zero entries, and the resulting system is commonly solved using specially-tailored block solvers reminiscent of the FEM frontal solvers. However, in this thesis, Eqn. 14 is solved iteratively region-by region until convergence is achieved, that is until the interfacial conditions in Eqn. 15 are satisfied. It is noted that in the case of perfect thermal contact $R_{t,c}^{"}(x_j) = 0$, and continuity of temperature is enforced.

Quadratic iso-parametric discontinuous boundary elements with nodes offset at 25% are used in all computations reported in this thesis (see Fig. 7).

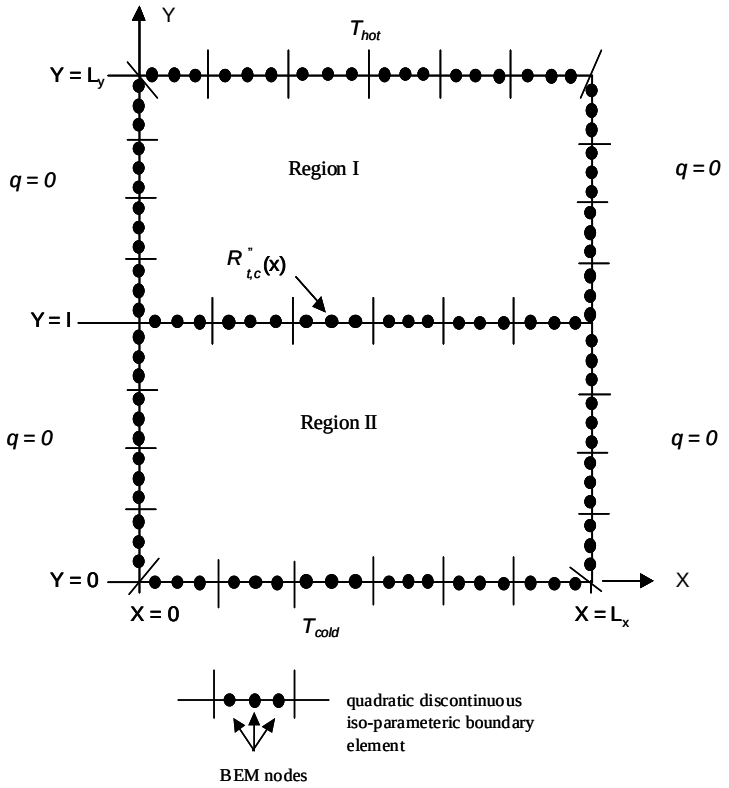

Figure 7. Boundary element model for the contact resistance problem

It should be noted that the Cartesian geometry adopted to model the test coupon in this thesis is chosen only for convenience, but any other simple geometry, such as axisymmetric test coupons, are readily modeled using BEM. The iteration process follows the initial step of guessing the interface conditions. In all examples reported in this thesis, an adiabatic condition $q^I = 0$ was arbitrarily imposed initially along the interface between the two regions. After the initial systems are formed and solved, mismatched temperatures are found along the interfaces for neighboring sub-domains. The interface temperatures are replaced for the average as:

$$T^I_{\Gamma \text{int}} = \frac{T^I_{\Gamma \text{int}} + T^{II}_{\Gamma \text{int}}}{2} + R''_{t,c} q^I_{\Gamma \text{int}} \tag{16}$$

the same search process is followed for the other side of the interface to produce the average as follows,

$$T_{\Gamma \text{int}}^{II} = \frac{T_{\Gamma \text{int}}^{I} + T_{\Gamma \text{int}}^{II}}{2} + R_{t,c}^{"} q_{\Gamma \text{int}}^{II} \tag{17}$$

where $R_{t,c}^{"}$ is the thermal contact resistance, $T_{\Gamma \text{int}}^{I}$ and $T_{\Gamma \text{int}}^{II}$ are the interfacial temperatures from region one and region two respectively, and $q_{\Gamma \text{int}}^{I}$ and $q_{\Gamma \text{int}}^{II}$ are the interfacial heat fluxes from region one and region two.

Once the resulting averaged temperatures are imposed as boundary conditions, a resulting set of normal heat fluxes along the interfaces will be matched from neighboring sub-domains requiring continuity as:

$$q_{\Gamma \text{int}}^{I} = q_{\Gamma \text{int}}^{I} - \frac{q_{\Gamma \text{int}}^{I} + q_{\Gamma \text{int}}^{II}}{2} \tag{18}$$

and,

$$q_{\Gamma \text{int}}^{II} = q_{\Gamma \text{int}}^{II} - \frac{q_{\Gamma \text{int}}^{I} + q_{\Gamma \text{int}}^{II}}{2} \tag{19}$$

to ensure the flux continuity condition $q_{\Gamma \text{int}}^{I} = -q_{\Gamma \text{int}}^{II}$ after averaging. The iteration process is continued until a convergence criterion is satisfied. A measure of convergence may be defined as the measure of mismatched temperatures along the interface as:

$$L_2 = \left\{ \frac{1}{2N_{\text{int}}} \left[\sum_{i=1}^{N_{\text{int}}} \left(T_{\Gamma \text{int}}^{I} - T_{u,\Gamma \text{int}}^{I} \right)^2 + \sum_{i=1}^{N_{\text{int}}} \left(T_{\Gamma \text{int}}^{II} - T_{u,\Gamma \text{int}}^{II} \right)^2 \right] \right\}^{\frac{1}{2}} \tag{20}$$

This is the standard deviation of BEM computed interface temperatures $T^{I}_{\Gamma \text{int}}$ on the region I side of the interface and $T^{II}_{\Gamma \text{int}}$ on the region II side of the interface and their averaged-out updated interface values $T^{I}_{\Gamma \text{int}}$,and $T^{II}_{\Gamma \text{int}}$, respectively given by Eqn. 15 and Eqn. 16. The iteration routine can be stopped once this standard deviation reaches a small fraction ε of ΔT (typically 10^{-6}), where ΔT is the total temperature span of the global field. It is shown in (Divo, 2002 #23) that the above iteration converges for jumps in interfacial temperature due to physically realistic values of the thermal contact resistance. Global iteration of the assembled BEM equations can be carried out alternatively using Newton-Raphson iteration.

CHAPTER SIX: TEST CASE SIMULATIONS

In this thesis, two sets of results are presented. The first obtained using the sensitivity based inverse problem method derived above and the second is using a regularized BEM/genetic algorithm (GA) numerical approach. In all test cases considered, the top and bottom regions are taken to be made of the same material, namely AISI 304 stainless steel with a constant conductivity value of 14.9 W/mK. Two cases of contact resistance are considered: (1) the first is constant, and (2) the second varies with position as $R''_{t,c}(x) = 0.0015 - 0.004x + 0.004x^2 + 0.00005\sin(4\pi x)\ Km^2/W$. The dimensions of the model are taken as $L_x = L_y = 0.1\ m$, the location of the contact region is taken as $l = 0.05\ m$. Nineteen equally spaced measuring points are located 0.00625 m above the interface region. The location of the measuring points was determined in a series of forward problems which examined the sensitivity of the temperature field to variations of the interface thermal contact resistance while still maintaining a physically realistic distance from the interface at which one could place sensors such as thin wire thermocouples in an actual experiment. Sensitivity maps are shown in Fig. 8 for two representative anchor point locations at the interface. It is clear that the measurement locations in this case should be placed as close to the contact interface as possible.

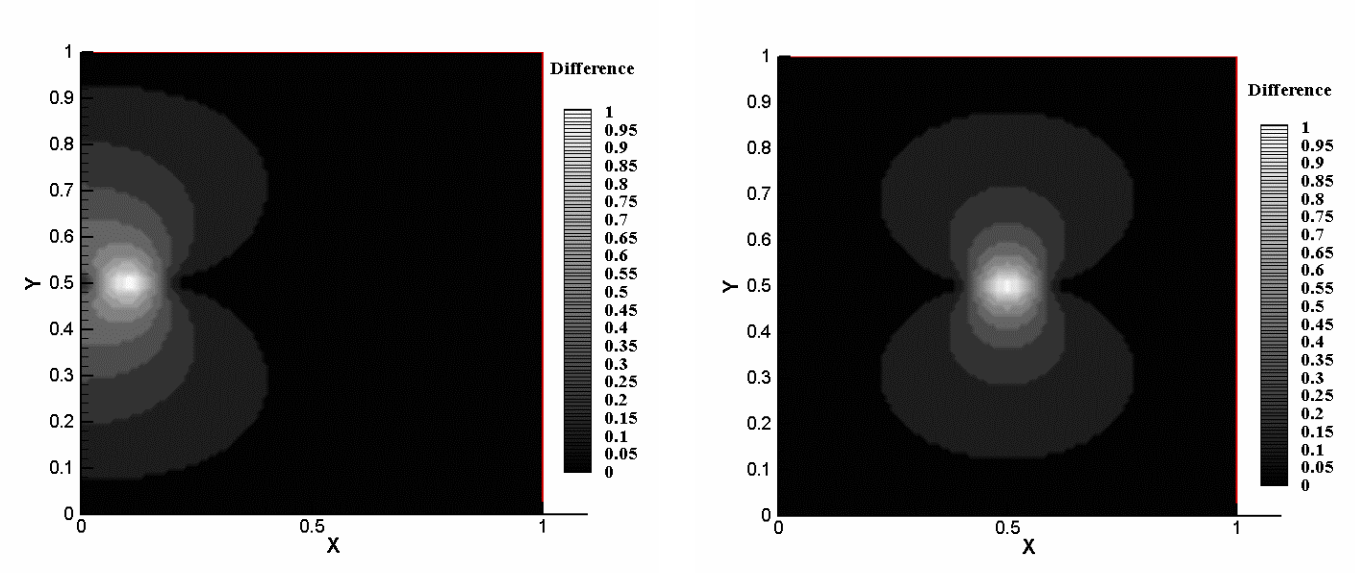

Figure 8. Sensitivity contour maps for the contact resistance problem

The resulting temperatures from the forward solution are considered as exact. In order to simulate error from the measurements, random noise is added to computed temperatures. Assuming measurement errors are additive, the measured temperatures are simulated as

$$T_{observed,j} = T_{BEM,j} + \in_j \tag{21}$$

where $T_{BEM,j}$ is the computed temperature at node *j* from the forward BEM solution. The additive error, $\in_j$, is produced by a random number generator, and its magnitude is controlled by the imposed standard deviation. Random error drawn from a normal distribution with a standard deviation of 0.25 K is then added to the temperatures at the measuring points. This value was chosen as being representative of experimental capability. The simulated error corresponds to

approximately a maximum of +/-0.64K for 99% of generated random errors. Several seeds were used to generate random numbers. The results are summarized in Table 1.

Table 1. Simulated observed temperatures for constant and variable $R''_{t,c}$.

	Input Temperature [K] at y = 0.05625 [m]			
	$R''_{t,c} = 0.0005\ Km^2/W$		$R''_{t,c} = 0.0015 - 0.004x + 0.004\,x^2 + 0.00005 \sin(4\pi x)\ Km^2/W$	
X/L	0 Error in Input [K]	+/- 0.64K Error Input	0 Error in Input [K]	+/- 0.64K Error Input
0.050	282.870	282.770	285.754	285.656
0.100	282.870	283.010	285.590	285.730
0.150	282.870	282.930	285.186	285.248
0.200	282.870	282.790	284.558	284.475
0.250	282.870	282.770	283.787	283.688
0.300	282.870	282.910	283.056	283.096
0.350	282.870	282.890	282.556	282.581
0.400	282.870	282.780	282.395	282.306
0.500	282.870	282.770	282.608	282.507
0.550	282.870	282.840	283.050	283.027
0.600	282.870	282.960	283.539	283.628
0.650	282.870	282.770	283.908	283.813
0.700	282.870	283.010	284.040	284.183
0.750	282.870	282.840	283.951	283.920
0.800	282.870	282.890	283.726	283.752
0.850	282.870	282.920	283.530	283.581
0.900	282.870	282.830	283.531	283.496
0.950	282.870	282.990	283.777	283.895
1.000	282.870	282.970	284.190	284.291

CHAPTER SEVEN: RESULTS FROM THE INVERSE ANALYSIS

In this chapter, two sets of results are presented in turn: (1) the sensitivity based approach, and (2) the BEM/GA based approach. In all cases the methodology of problem simulations described in chapter 6 is followed.

The Sensitivity-Based Results

Fig. 9 shows the result for the constant resistance case and the straightforward inversion of Eqn. 1 with no simulated input errors. It can be seen that the values are non-physical at the center with a very large error.

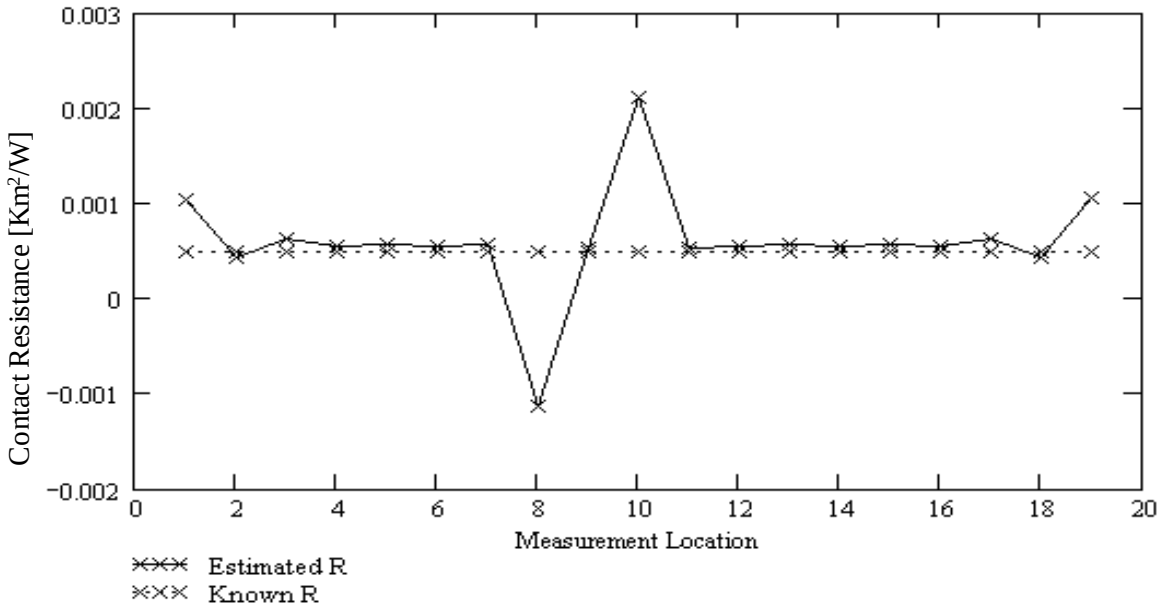

Figure 9. $R''_{t,c}$ = 0.0005 K m^2/W. No error was added to simulated temperature readings.

The standard root mean square (RMS) error between the known resistance and the calculated resistance is 2.4×10^{-4} Km^2/W. This unacceptable result is due to round off error in the values of the sensitivity matrix and the inherent stiffness of the matrix. To get around this problem the regularization method was applied using Eqn. 11. The results are shown in Fig. 10. It can be seen that the results are realistic. The choice of the regularization parameter by the L-curve will be illustrated in the next section where the BEM/GA results are presented. The RMS error between the estimated and the known resistance is 9.965×10^{-5} Km^2/W. Although the RMS only improved by a factor of two, the impact of the regularization is apparent in comparing Fig. 9 and Fig. 10.

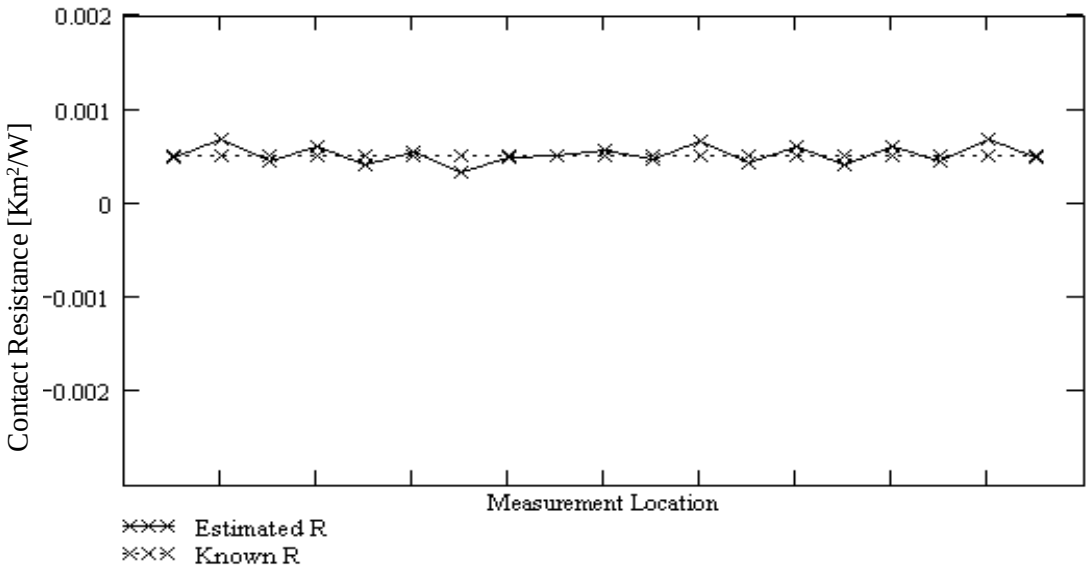

Figure 10. $R''_{t,c} = 0.0005$ K m^2/W. Regularized inverse solution.

For the variable contact resistance case, the results are shown in Fig. 11 and Fig. 12. It can be seen that the results are realistic and have an RMS error of 2.38×10^{-4} Km^2/W. As can be seen in Fig 10 and Fig. 12 the result is insensitive to noise.

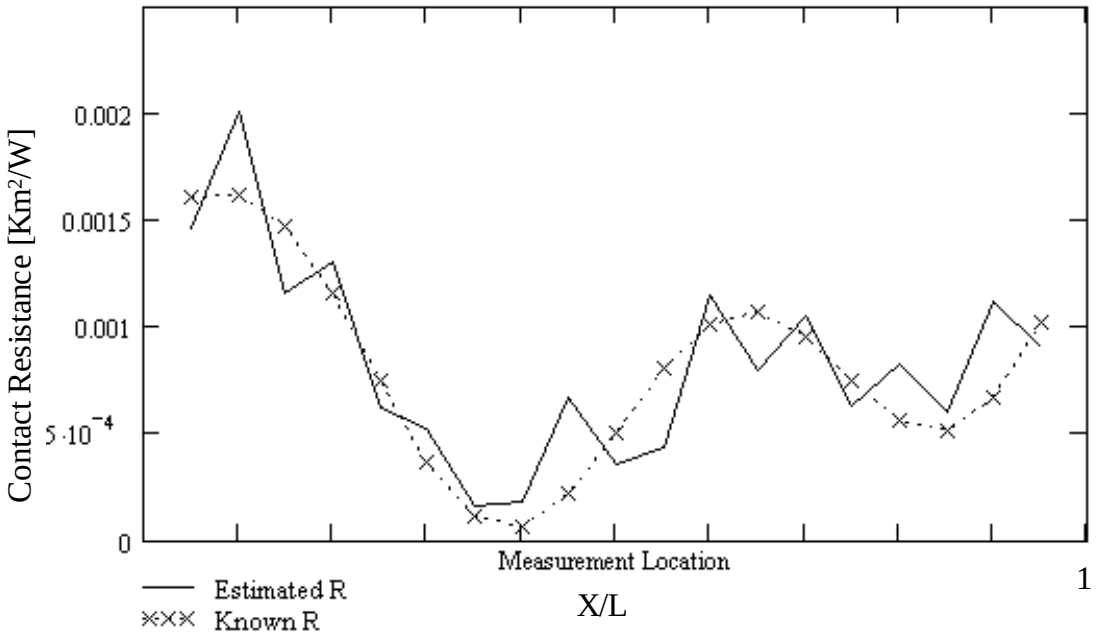

Figure 11. Regularized inverse solution for exact inputs for $R''_{t,c}(x) = 0.0015 - 0.004x + 0.004x^2 + 0.00005\sin(4\pi x)\ Km^2/W$.

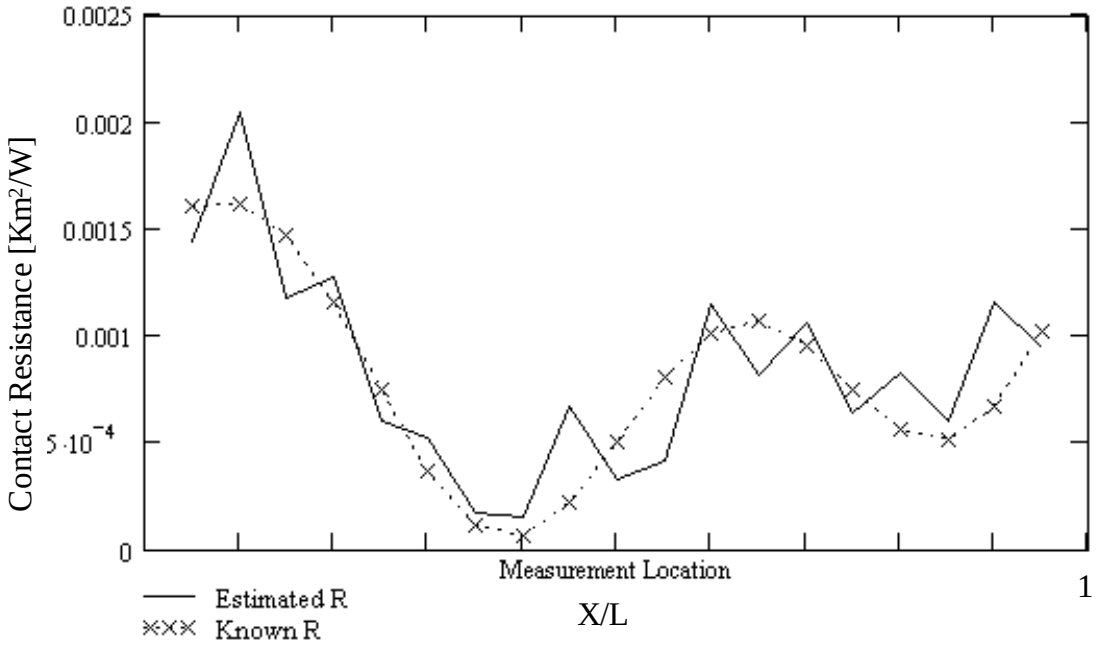

Figure 12. $R_{t,c}^{*}(x) = 0.0015 - 0.004x + 0.004x^2 + 0.00005\sin(4\pi x)\ Km^2/W$. Regularized inverse solution with noise, the error in the estimated resistance only increases to 2.45 x 10^{-4}Km^2/W.

The BEM/GA-Based Results

In the GA we used to generate results presented in the example section, the following parameters are chosen: population size of 10 individuals/generation, with a string of ten bits to define each parameter within each individual, two children per mating, a 1% probability of mutation, and a 70% probability of crossover. The population is not allowed to grow. This combination of parameters has been proven to yield efficient and accurate optimization results for different studies carried out by the authors Divo et al (2002).

The BEM discretization is shown in Fig. 13. A (1x1) Square with boundary conditions as shown with each of the two regions are discretized with 30 quadratic isoparametric discontinuous elements. There are 19 sensor locations at $x:(0.05,\ 0.1,\ ...,\ 0.95)$ and $y:(0.5625)$. There are 11 anchor points at $x:(0,\ 0.1,\ ...,\ 1)$ and $y:(0.5)$. The genetic algorithm uses anchor points to parameterize the contact resistance function at the mating surface.

Results from the first case, $R''_{t,c} = 0.0005\ Km^2/W$, are plotted in Fig. 13. Anchor points are used to determine $R''_{t,c}$.

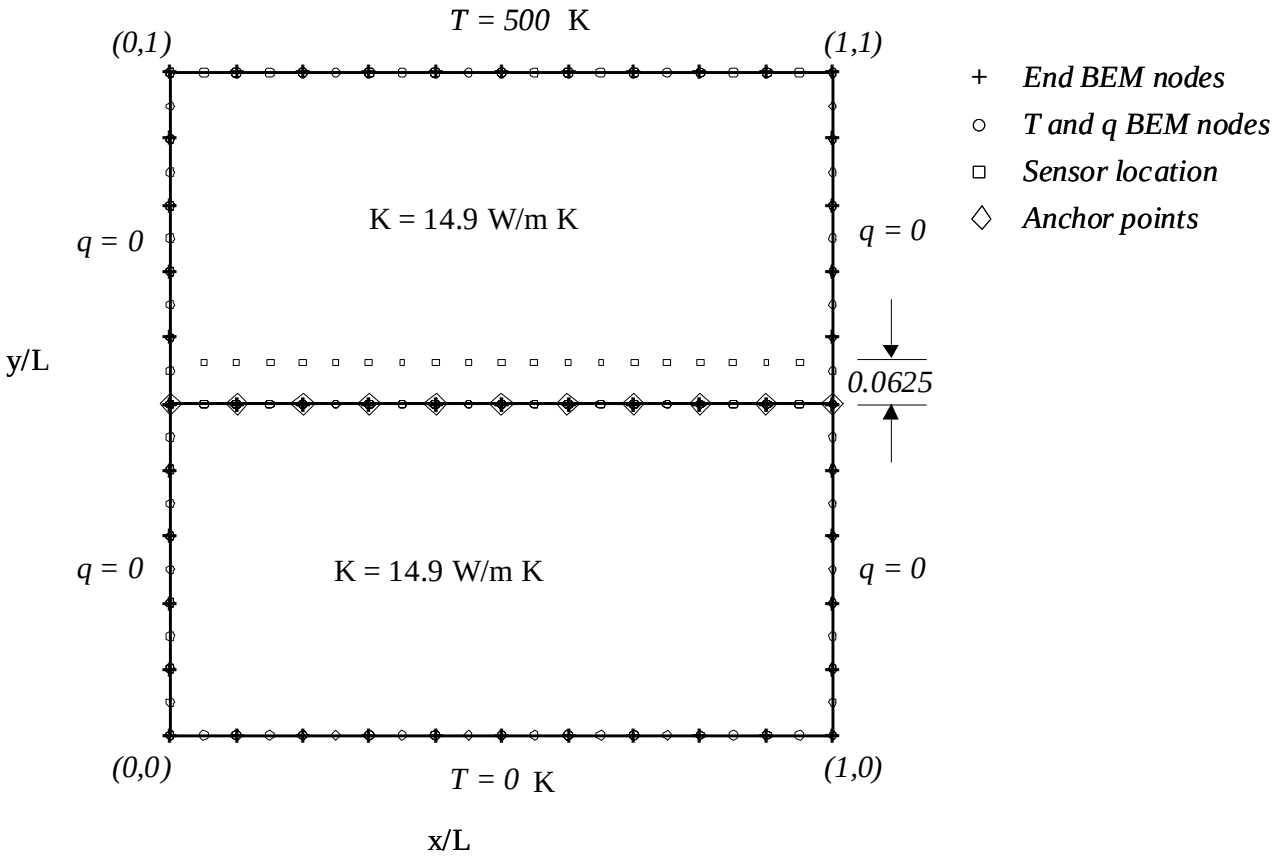

Figure 13. BEM discretization, boundary conditions, and inverse problem setup

With exact temperatures input at the measuring points, the contact resistance is accurately retrieved. Random error drawn from a normal distribution with a standard deviation of 0.25 K is then added to the temperatures at the measuring points. The simulated error corresponds to approximately a maximum of 0.64 for 99% of generated random errors. Several seeds were used to generate random numbers.

The results shown in Fig. 14 are for a value of β equal to 0.0005. This results in a RMS error of 1.8 x 10^{-7} Km^2/W, which is lower than the errors computed for the original objective function, i.e. $\beta = 0$ where the RMS error is 8 x 10^{-6} Km^2/W. Fig. 15 shows the effect of noise added to the simulated thermocouple readings. In this case, with $\beta = 0.0005$, the RMS error increased to 5.7 x 10^{-6} Km^2/W, which is still better than $\beta = 0$, which yields a RMS error of 8.6 x 10^{-6} Km^2/W. It is interesting to note that the apparent randomness in Fig. 14 is lost in Fig. 15 when the noise was added. However the points are not in a symmetric pattern and are distributed both above and below the known resistance, suggesting that it is indeed random.

Next, the case of variable contact resistance is considered:

$R''_{t,c}(x) = 0.0015 - 0.004x + 0.004x^2 + 0.00005\sin(4\pi x)\ Km^2/W$. Here one level of random error is introduced and added to the computed temperatures at the measuring points. These errors are normally distributed with a maximum of ± 0.5 for 99% of generated random errors.

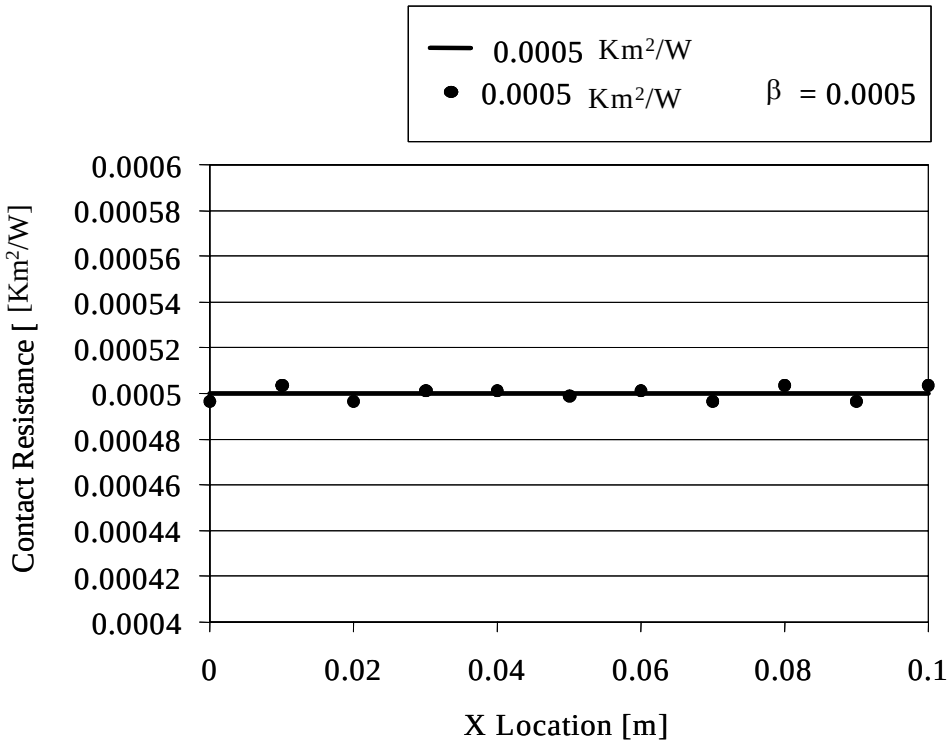

Figure 14. Results for case of $R_{t,c}^{"} = 0.0005\ Km^2/W$

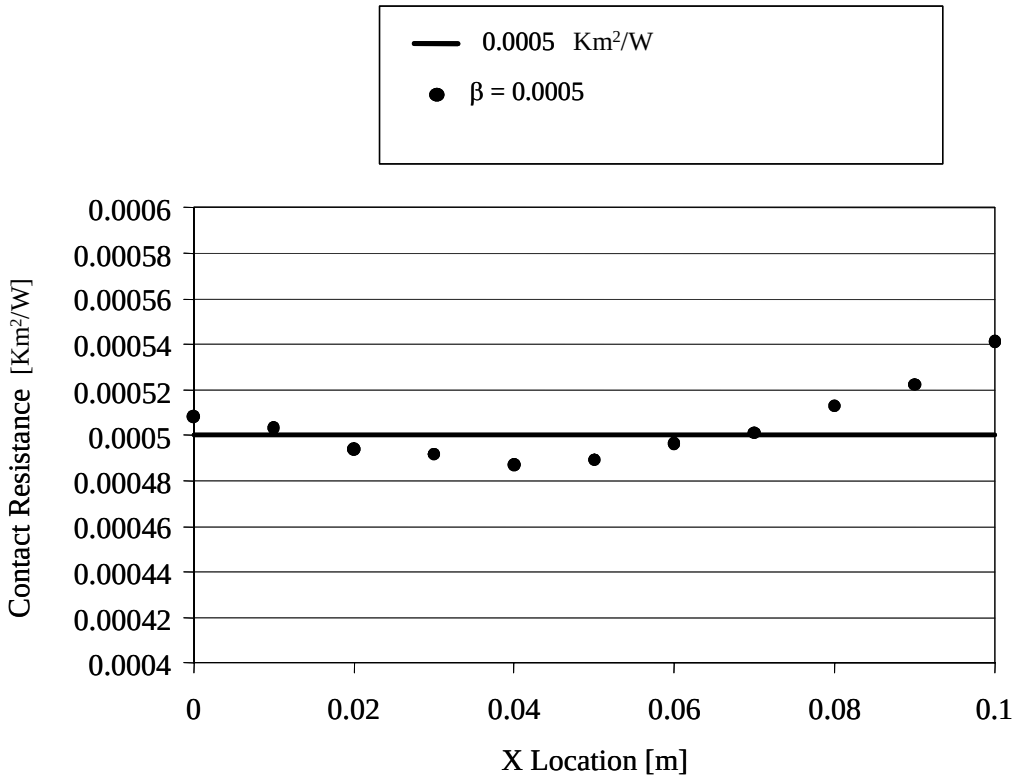

Figure 15. $R_{t,c}^{"} = 0.0005\ Km^2/W$ case with random noise

The algorithm is able to retrieve an accurate distribution for the contact resistance. In the case of no simulated input error, Fig. 16, input temperatures the algorithm retrieves $R_{t,c}^{"}(x)$ with a relative error of 6.1 x 10^{-5} Km^2/W, using $\beta = 0.0002$. The error computed for the original objective function, i.e. $\beta = 0$ is 7 x 10^{-5} Km^2/W. For the case of variable contact resistance with noise, the relative error (Fit2) was computed as 0.32 Km^2/W, using $\beta = 0$; 0.27 Km^2/W for $\beta = 0.001$; and 0.22 Km^2/W for $\beta = 0.01$. Fig. 17 shows the effect of noise in the thermocouple readings on the retrieved thermal contact resistance.

In all cases studied, the modified objective function yielded better results for resistance provided a proper value of β was chosen. The method used to choose β was based on the L

curve technique (Hansen, 1992; Hansen and O'Leary 1993). The value of β is an important parameter in the process. In this method, the choice of the value of β involves comparing the residuals in the minimum of the first term of Eqn. 5 (Fit1), which is the residuals in the temperatures, to the residuals in the second term of Eqn. 5 (Fit2) which represents the residuals in the resistance. These are shown in Fig. 18 and Fig. 19, for a range of β from 0 to 1. These fits are a function of a value of β chosen for the process. The desired value of β minimizes the residuals and maintains them equally balanced between both terms. In the case of the contact resistance variation of $R''_{t,c}(x) = 0.0015 - 0.004x + 0.004x^2 + 0.00005\sin(4\pi x)\ Km^2/W$, the optimal value of β is chosen to be 0.002. It is worth noting, the competing relation between Fit1 and Fit2: as Fit2 is driven down, Fit1 will increase, and this is clearly seen in Figs. 18 and 19.

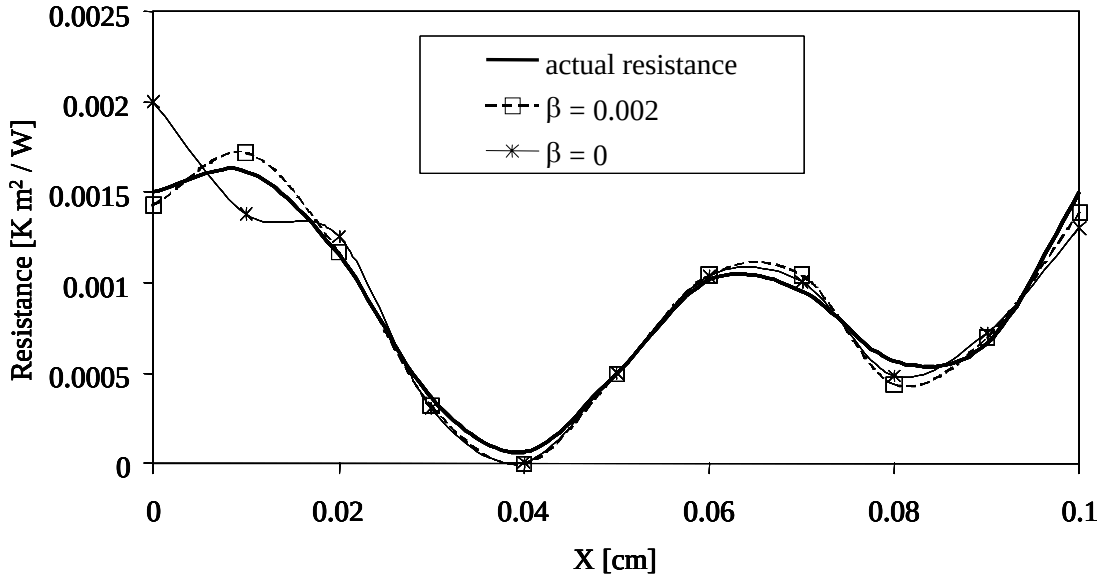

Figure 16. Plot of the variable thermal contact resistance case, eleven anchor points, and after 3000 iterations. The resistance is
$R''_{t,c}(x) = 0.0015 - 0.004x + 0.004x^2 + 0.00005\sin(4\pi x)\ Km^2/W$.

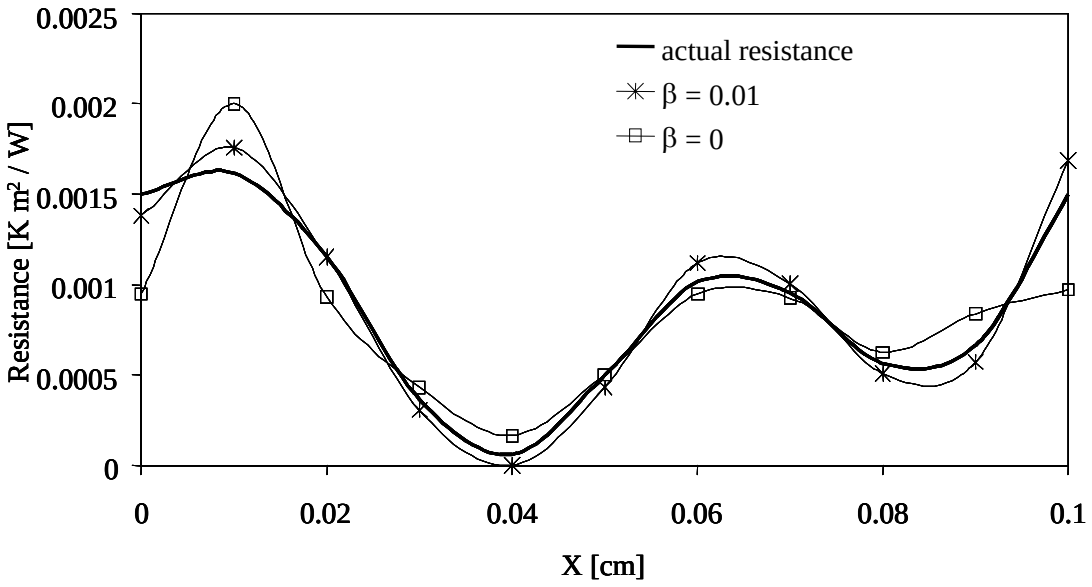

Figure 17. Plot of the variable resistance case, with random errors added to exact input temperatures. Results after 3000 iterations of the GA for the contact resistance.
$R''_{t,c}(x) = 0.0015 - 0.004x + 0.004x^2 + 0.00005\sin(4\pi x)\ Km^2/W$

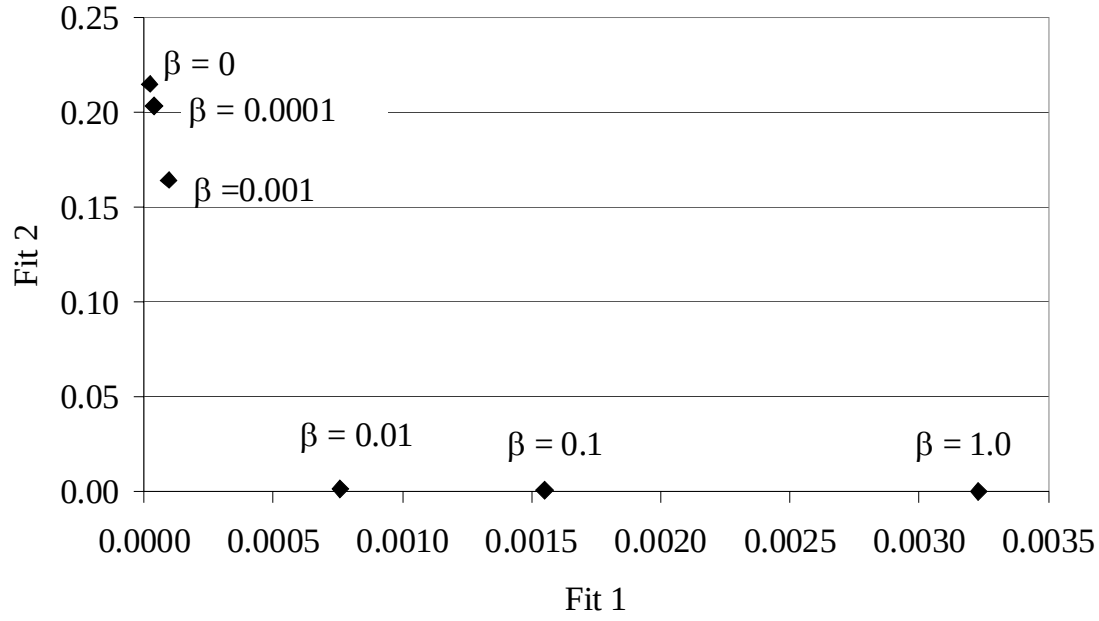

Figure 18. L curve for the contact resistance variation of $R_{t,c}^{"}(x) = 0.0015 - 0.004x + 0.004x^2 + 0.00005\sin(4\pi x)\ Km^2/W$.

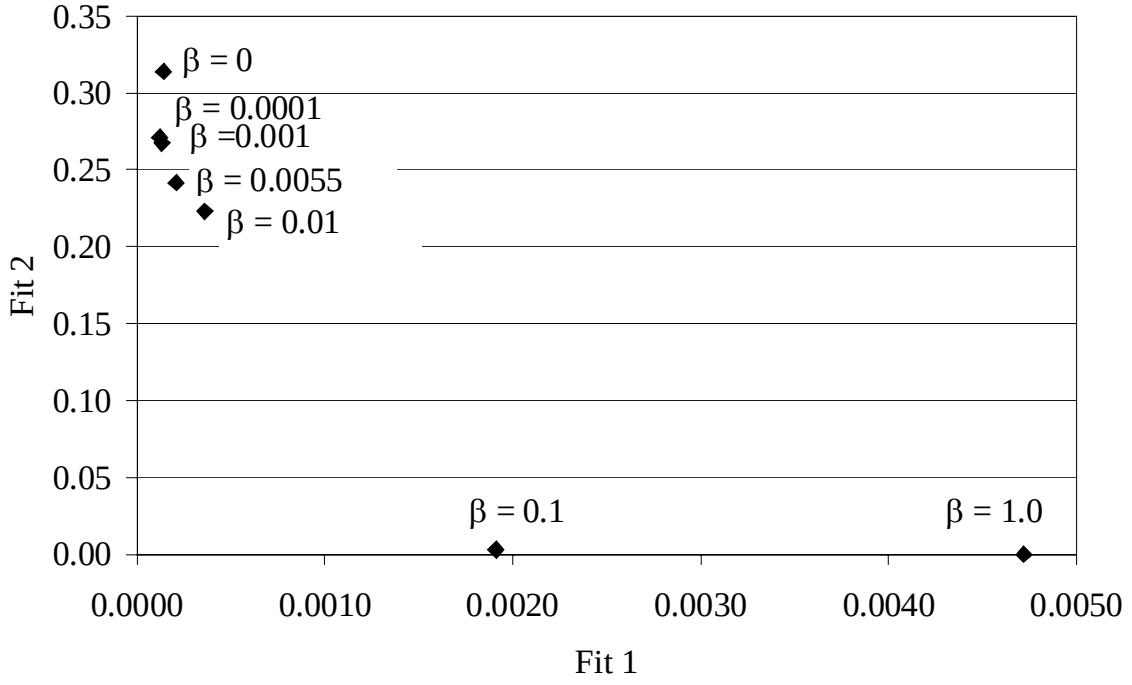

Figure 19. L curve for the contact resistance variation of $R''_{t,c}(x) = 0.0015 - 0.004x + 0.004x^2 + 0.00005\sin(4\pi x)\ Km^2/W$. A simulated noise error with a standard deviation of +/-0.25K was added for this case.

CHAPTER EIGHT: CONCLUSION

A two dimensional contact resistance model problem has been solved analytically for a known contact resistance between two mated surfaces. An inverse problem was then formulated to estimate the spatial variation of the contact resistance by using specific interior temperature measurement points. It was found that the inverse problem is sensitive to noise and requires using a regularization technique to obtain physically possible results. A variation of the Thikonov regularization method along with the L-curve was employed to determine the optimal regularization parameter value. A sensitivity based method was devised for linear problems while the regularization technique was then extended to a BEM/genetic algorithm to perform the inverse analysis for more general cases. Numerical simulations were carried out to demonstrate the approach. Random noise was used to simulate the effect of input uncertainties in measured temperatures at the sensors. It was demonstrated that the regularization technique for the genetic algorithm consistently provided in an improved result. Even though the cases presented here showed only a slight improvement, it is worth noting when working with real data one seeks the best method.

APPENDIX: ANALYTICAL SOLUTION

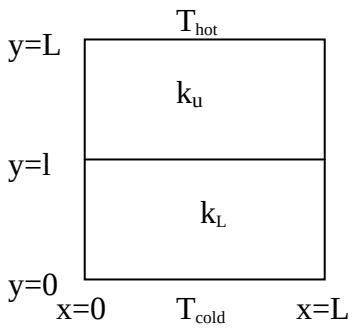

Figure 20. Nomenclature used in deriving the analytical solution.

The governing equations for the upper and bottom regions of the model problem are:

$$\nabla^2 T_u = 0$$
$$\nabla^2 T_b = 0 \qquad \text{(1A)}$$

The boundary conditions are:

$$\text{BC 1)} \quad \frac{\partial T_U}{\partial x}(0,y) = \frac{\partial T_U}{\partial x}(L,y) = \frac{\partial T_b}{\partial x}(0,y) = \frac{\partial T_b}{\partial x}(L,y) = 0 \qquad \text{(2A)}$$

$$\text{BC 2)} \quad k_U \frac{\partial T_U}{\partial y}(x,y) = k_b \frac{\partial T_b}{\partial y}(x,y)\Big|_{y=l} \qquad \text{(3A)}$$

The variation of the contact resistance is taken as a general function of space

$$R(x) = f(x) \qquad \text{(4A)}$$

The ratio of conductivities of the upper and bottom regions is

$$k_r = \frac{k_u}{k_b} \tag{5A}$$

and the eigen-values of the homogeneous problem are denoted by

$$\lambda_n = n\pi \tag{6A}$$

A separation of variables solution for each region with the boundary conditions 2A and 3A applied leads to the following temperature expressions for the top and bottom regions:

$$T_u(x,y) = (T_{hot} - T_{cold})\left[1 - \frac{c_0}{k_r}\left(1 - \frac{y}{l}\right) - \sum \frac{c_n}{k_r}\cos\left(\lambda_n \frac{x}{L}\right)\sinh\left(\lambda_n - \lambda_n \frac{y}{L}\right)\right] \tag{7A}$$

$$T_b(x,y) = (T_{hot} - T_{cold})\left[c_0 \frac{y}{l} + \sum c_n \cos\left(\lambda_n \frac{x}{L}\right)\sinh\left(\lambda_n \frac{y}{L}\right)\right] \tag{8A}$$

Imposing the temperature jump condition at the interface of the top and bottom regions leads to:

$$\text{BC 3)} \quad R(x) k_b \frac{\partial T_b}{\partial y}(x,y)\bigg|_{y=l} = T_u(x,y) - T_b(x,y)\big|_{y=l} \tag{9A}$$

which collapses to a continuity condition of $R(x) = 0$ that is, $T_u(x,y) = T_b(x,y)\big|_{y=l}$, in such a case. Using BC3 to find c_0:

$$\frac{\partial T_b}{\partial y}(x,y) = (T_{hot} - T_{cold})\left[\frac{c_0}{L} + \sum \frac{c_n \lambda_n}{L}\cos\left(\lambda_n \frac{x}{L}\right)\cosh\left(\lambda_n \frac{y}{L}\right)\right] \tag{10A}$$

$$k_b \frac{\partial T_b}{\partial y}(x,l) = (T_{hot} - T_{cold})\left[\frac{c_0 k_b}{L} + \sum \frac{c_n \lambda_n k_b}{L}\cos\left(\lambda_n \frac{x}{L}\right)\cosh\left(\lambda_n \frac{l}{L}\right)\right] \tag{11A}$$

so:

$$R(x)(T_{hot}-T_{cold})k_b\left[\frac{c_0}{L}+\sum\frac{c_n\lambda_n}{L}\cos\left(\lambda_n\frac{x}{L}\right)\cosh\left(\lambda_n\frac{l}{L}\right)\right]$$
$$=(T_{hot}-T_{cold})\left[1-\frac{c_0}{k_r}\left(1-\frac{l}{L}\right)-\sum\frac{c_n}{k_r}\cos\left(\lambda_n\frac{x}{L}\right)\sinh\left(\lambda_n-\lambda_n\frac{l}{L}\right)\right] \quad (12A)$$
$$-(T_{hot}-T_{cold})\left[c_0\frac{l}{L}+\sum c_n\cos\left(\lambda_n\frac{x}{L}\right)\sinh\left(\lambda_n\frac{l}{L}\right)\right]$$

Re-arranging gives:

$$\frac{R(x)k_b}{L}c_0+\frac{R(x)k_b}{L}\left[\sum c_n\lambda_n\cos\left(\lambda_n\frac{x}{L}\right)\cosh\left(\lambda_n\frac{l}{L}\right)\right]$$
$$=1-\frac{c_0}{k_r}\left(1-\frac{l}{L}\right)-\sum\frac{c_n}{k_r}\cos\left(\lambda_n\frac{x}{L}\right)\sinh\left(\lambda_n-\lambda_n\frac{l}{L}\right) \quad (13A)$$
$$-c_0\frac{l}{L}-\sum c_n\cos\left(\lambda_n\frac{x}{L}\right)\sinh\left(\lambda_n\frac{l}{L}\right)$$

Multiply Eqn 13A by dx and integrate from 0 to L:

$$\int_0^L R(x)dx\frac{k_b}{L}c_0=L-\frac{c_0L}{k_r}\left(1-\frac{l}{L}\right)-c_0\frac{l}{L}L \quad (14A)$$

$$c_0\left(k_b\frac{\int_0^L R(x)\,dx}{L}+\frac{L}{k_r}\left(1-\frac{l}{L}\right)+l\right)=L \quad (15A)$$

Solving for c_0:

$$c_0 = \frac{L}{k_b \frac{\int_0^L R(x)\,dx}{L} + \frac{k_b}{k_u}\left(1 - \frac{l}{L}\right) + \frac{l}{L}} \tag{16A}$$

Check if $R(x) = 0$ and $k_r = 1$.

$$c_0 = \frac{1}{1 - \frac{l}{L} + \frac{l}{L}} = 1 \tag{17A}$$

To get c_n from Eqn. 13A, multiply by $\cos\left(\lambda_n \frac{x}{L}\right)$ and integrate 0 to L.

$$k_b c_0 \int_0^L R(x)\cos\left(\lambda_n \frac{x}{L}\right)dy + \frac{k_b}{L}\left(\sum \cosh\left(\lambda_n \frac{l}{L}\right) c_n \lambda_n II_{n,m}\right) \tag{18A}$$

$$= c_o \, \mathrm{I}_m + \sum c_n \lambda_n \cosh\left(\lambda_n \frac{l}{L}\right) II_{n,m}$$

where:

$$I_m = k_b \int_0^L R(x)\cos\left(\lambda_m \frac{x}{L}\right)dx \tag{19A}$$

$$II_{n,m} = \frac{k_b \int_0^L \cos\left(\lambda_n \frac{x}{L}\right)\cos\left(\lambda_m \frac{x}{L}\right)}{L} R(x)\,dx \tag{20A}$$

The problem is how to isolate an expression for c_m when it is buried in the summation term. The solution is to recast the equation in a matrix form, for example for x/L=0.5:

$$c_0 \cdot \begin{bmatrix} 0 \\ 0 \\ I_m \\ 0 \end{bmatrix} + \begin{bmatrix} II_{11} & II_{12} & II_{1m} & II_{14} \\ II_{21} & II_{22} & II_{2m} & II_{24} \\ II_{m1} & II_{m2} & II_{mm} & II_{m4} \\ II_{41} & II_{42} & II_{43} & II_{44} \end{bmatrix} \cdot \begin{bmatrix} \lambda_1 \cosh(0.5 \cdot \lambda_1) \cdot c_1 \\ \lambda_2 \cosh(0.5 \cdot \lambda_2) \cdot c_2 \\ \lambda_m \cosh(0.5 \cdot \lambda_m) \cdot c_m \\ \lambda_4 \cosh(0.5 \cdot \lambda_4) \cdot c_4 \end{bmatrix} = \begin{bmatrix} 0 \\ 0 \\ -\frac{1}{2} \cdot c_m \cdot \left(\frac{1}{k_R} + 1 \right) \cdot \sinh(0.5 \cdot \lambda_n) \\ 0 \end{bmatrix} \tag{21A}$$

Note that we are considering only the first 4 terms in the series to show how the approach works. In reality there are an infinite number of terms and the matrices have an infinite number of elements. In the analysis we used about 20 terms in the series and the matrices were 1x20 and 20x20.

Forming the inverse for the II matrix

$$\overline{E} = II^{-1} \tag{22A}$$

And multiplying the inverse through the equation gives

$$\overline{E} \cdot c_0 \cdot \begin{bmatrix} 0 \\ 0 \\ I_m \\ 0 \end{bmatrix} + \begin{bmatrix} 1 & 0 & 0 & 0 \\ 0 & 1 & 0 & 0 \\ 0 & 0 & 1 & 0 \\ 0 & 0 & 0 & 1 \end{bmatrix} \cdot \begin{bmatrix} \lambda_1 \cdot \cosh(0.5 \cdot \lambda_1) \cdot c_1 \\ \lambda_2 \cdot \cosh(0.5 \cdot \lambda_2) \cdot c_2 \\ \lambda_m \cdot \cosh(0.5 \cdot \lambda_m) \cdot c_m \\ \lambda_4 \cdot \cosh(0.5 \cdot \lambda_4) \cdot c_4 \end{bmatrix} = \overline{E} \cdot \begin{bmatrix} 0 \\ 0 \\ -\frac{1}{2} \cdot c_m \cdot \left(\frac{1}{k_R} + 1 \right) \cdot \sinh(0.5 \cdot \lambda_n) \\ 0 \end{bmatrix} \tag{23A}$$

When expanded out this results in 4 equations. Each equation will involve c_0, one of the c's, one of the elements of E and one of the λ's.

$$E_{m1} \cdot c_0 I_m + \lambda_1 \cdot \cosh(0.5 \cdot \lambda_1) \cdot c_1 = -E_{m1} \cdot \frac{c_1}{2} \cdot \left(\frac{1}{K_R} + 1 \right) \cdot \sinh(0.5 \cdot \lambda_1) \quad \text{(24A)}$$

$$E_{m2} \cdot c_0 I_m + \lambda_2 \cdot \cosh(0.5 \cdot \lambda_2) \cdot c_2 = -E_{m2} \cdot \frac{c_2}{2} \cdot \left(\frac{1}{K_R} + 1 \right) \cdot \sinh(0.5 \cdot \lambda_2) \quad \text{(25A)}$$

$$E_{mm} \cdot c_0 I_m + \lambda_m \cdot \cosh(0.5 \cdot \lambda_m) \cdot c_m = -E_{mm} \cdot \frac{c_1}{2} \cdot \left(\frac{1}{K_R} + 1 \right) \cdot \sinh(0.5 \cdot \lambda_m) \quad \text{(26A)}$$

$$E_{m4} \cdot c_0 I_m + \lambda_4 \cdot \cosh(0.5 \cdot \lambda_4) \cdot c_1 = -E_{m4} \cdot \frac{c_4}{2} \cdot \left(\frac{1}{K_R} + 1 \right) \cdot \sinh(0.5 \cdot \lambda_4) \quad \text{(27A)}$$

We are only interested in the third equation that involves E_{mm}. That equation allows us to solve for c_m directly without knowing any of the other c's. This approach can be generalized to many terms; the addition of terms changes the values of the inverse elements and hence affects the values of the c's.

LIST OF REFERENCES

1. DeVaal, J.W., Yovanovich, M.M., and Negus, K., 1987, "The Effects of Surface Slope Anisotropy on the Contact Conductance of Conforming Rough Surfaces," *Proceedings of the ASME Symposium on Developments in Contact Resistance*, ASME National Heat Transfer Conference, Pittsburgh, P.A., pp. 123-134.
2. Negus, K.J., Vaoverbeke, C.A., and Yovanovich, M.M., 1987, "Thermal Constriction Resistance with Variable Thermal Conductivity Near the Contact Surface," *Proceedings of the ASME Symposium on Developments in Contact Resistance*, ASME National Heat Transfer Conference, Pittsburgh, P.A., pp. 91-98.
3. Muzychka,Y.S., Sridhar, M.R., and Yovanovich, M.M., 1996, "Thermal Constriction Resistance in Multi-layer Contacts: application in thermal contact rsesistance" *AIAA Paper* 96-3967.
4. Marotta, E.E., and Fletcher, L.S., 2001, "Thermal Contact Resistance Modeling of Non-flat, Roughened Surfaces with Non-Metallic Coatings," *ASME Journal of Heat Transfer*, Vol. 123, pp. 11- 23.
5. Yovanovich, M.M., 1998, "Chapter 3: Conduction and Thermal Contact Resistance (conductance)," in *Handbook of Heat Transfer*, W.M. Rosenhow, J.P. Harnett, and Y.L. Cho, eds., McGraw Hill Book Co., New York.
6. Fletcher,L.S., "Recent Developments in Contact Conductance Heat Transfer," *ASME Journal of Heat Transfer*, Vol. 110, pp. 1059-1070.

7. Madhusudana, C.V. and Fletcher, L.S., 1986, "Contact Heat Transfer - the last decade, " *AIAA Journal*, Vol. 24, No3., pp. 510-523.
8. Blackwell, B., Gill, W., Dowding, K.J., and Voth, T., 2000, "Determination of Thermal Conductivity of 304 Stainless Steel Using Parameter Estimation Techniques," *ASME Paper NHTC2000-12141*.
9. Beck, J.V., Blackwell, B., and St. Clair, C.R., *Inverse Heat Conduction: Ill-Posed Problems*, John Wiley and Sons, New York, 1985.
10. Alifanov, O., 1994, *Inverse Heat Transfer Problems*, Springer-Verlag, New York.
11. Kurpisz, K. and Nowak, A.J., 1995, *Inverse Thermal Problems*, Computational Mechanics, Billerica.
12. Blackwell, B., and Dowding, K.J., 2002, "Sensitivity and Uncertainty Analysis for Thermal Problems," *4th International Conference on Inverse Problems in Engineering*, Rio de Janeiro, Brazil.
13. Bialecki, R., Divo, E., and Kassab, A.J., 2003, "Explicit Calculation of Smoothed Sensitivity Coefficients for Linear Problems," *International Journal for Numerical Methods in Engineering*, Vol. 57, pp. 143-167.
14. Brebbia, CA., Telles, J.C.F., and Wrobel, L., 1985, *Boundary Element Techniques in Engineering*, Springer-Verlag, New York.
15. Kassab, A.J. and Wrobel, L.C., 2000, "Boundary Element Methods in Heat Conduction," *Chapter 5 in Recent Advances in Numerical Heat Transfer*, W.J. Mincowycz and E. M. Sparrow, (eds.), Vol. 2, Taylor and Francis, New York, 2000, pp. 143-188.

16. Divo, E. and Kassab, A.J., 1997, "A Boundary Integral Equation for Steady Heat Conduction in Anisotropic and Heterogeneous Media," *Num. Heat Transfer, Part B: Fundamentals*, Vol. 32, No. 1, pp. 37-61.

17. Divo, E. and Kassab, A.J., 1998, "A Generalized BIE for Transient Heat Conduction in Heterogeneous Media,"*J. Thermophysics and Heat Transfer*, Vol. 12, No. 3, pp. 364-373.

18. Kassab, A.J., Wrobel, L.C., Bialecki, R., and Divo, E., "Boundary Elements Method," Chapter 6 in *Handbook Of Numerical Heat Transfer*, 2nd Edition, Minkowycz, W., Sparrow, E.M., and Murthy, J. Y. (eds.), John Wiley and Sons, 2004.

19. Divo, E. and Kassab, A.J., *Boundary Element Method for Heat Conduction with Applications in NonHomogeneous Media*, Wessex Institute of Technology (WIT) Press, Southampton, UK, and Boston, USA, 2003.

20. Goldberg, D.E., *Genetic Algorithms in Search, Optimization and Machine Learning*, Addison-Wesley, Reading, MA, 1989.

21. Divo, E., Kassab, A.J., and Gill, J., 2002, "An Inverse Algorithm to Estimate Spatially Varying Contact Resistance," *ASME Paper IMECE2002-32429*.

22. Hansen, P. C., and O'Leary, D., 1993, "The Use of the L-Curve in the Regularization of Discrete Ill-Posed Problems,"*SIAM J. Sci. Comput*., Vol. 14, No.6, pp.1487-1503.

23. Hansen, C., 1992, "Analysis of Discrete Ill-Posed Problems by Means of theL-Curve," *SIAM Review*, Vol. 34, No. 4, pp. 561-580.

24. Thikonov, A. and Arsenin, V., 1977, Solution of Ill-Posed Problems, John Wiley and Sons, New York.

25. Beck, J.V., Blackwell, B., and St. Clair, C.R.,1985, Inverse Heat Conduction: Ill -Posed Problems, John Wiley and Sons, New York.

26. Alifanov, O., 1994, Inverse Heat Transfer Problems, Springer-Verlag, New York.

27. Kurpisz, K. and Nowak, A.J., 1995, InverseThermal Problems, Computational Mechanics, Boston.

28. Zhang, F., Kassab, A.J., and Nicholson, D.W., "A Boundary Element Solution of an Inverse Elasticity Problem and Applications to Determining Residual Stress and Contact Stress," *International Journal of Solids and Structures*, Vol. 34, No.16, 1997, pp. 2073-2086.